

Not Just Pretty Pictures: Text-to-Image Generators Enable Interpretable Interventions for Robust Representations

Jianhao Yuan^{†*} Francesco Pinto^{†*} Adam Davies[‡] Aarushi Gupta[◇] Philip Torr[†]

[†]University of Oxford [‡]University of Illinois Urbana-Champaign [◇]Indian Institute of Technology, Delhi

Abstract

Neural image classifiers are known to undergo severe performance degradation when exposed to input that exhibits covariate-shift with respect to the training distribution. Successful hand-crafted augmentation pipelines aim at either approximating the expected test domain conditions or to perturb the features that are specific to the training environment. The development of effective pipelines is typically cumbersome, and produce transformations whose impact on the classifier performance are hard to understand and control. In this paper, we show that recent Text-to-Image (T2I) generators' ability to simulate image interventions via natural-language prompts can be leveraged to train more robust models, offering a more interpretable and controllable alternative to traditional augmentation methods. We find that a variety of prompting mechanisms are effective for producing synthetic training data sufficient to achieve state-of-the-art performance in widely-adopted domain-generalization benchmarks and reduce classifiers' dependency on spurious features. Our work suggests that further progress in T2I generation and a tighter integration with other research fields may represent a significant step towards the development of more robust machine learning systems.

1. Introduction

The success of deep neural classifiers is largely built on the assumption that the train and test data are identically and independently distributed (i.i.d.). In real-world applications, slight changes in the environmental conditions in which the image is captured can break this assumption. Since these changes only affect the inputs (i.e., the covariates) without altering the labels, this form of distribution shift is also known as covariate-shift [41], and it has been observed to significantly hurt accuracy [17, 57]. For instance, neural networks trained on images collected in

*Equal contribution. Corresponding authors details: yuanjianhao2019@gmail.com; francesco1.pinto@gmail.com

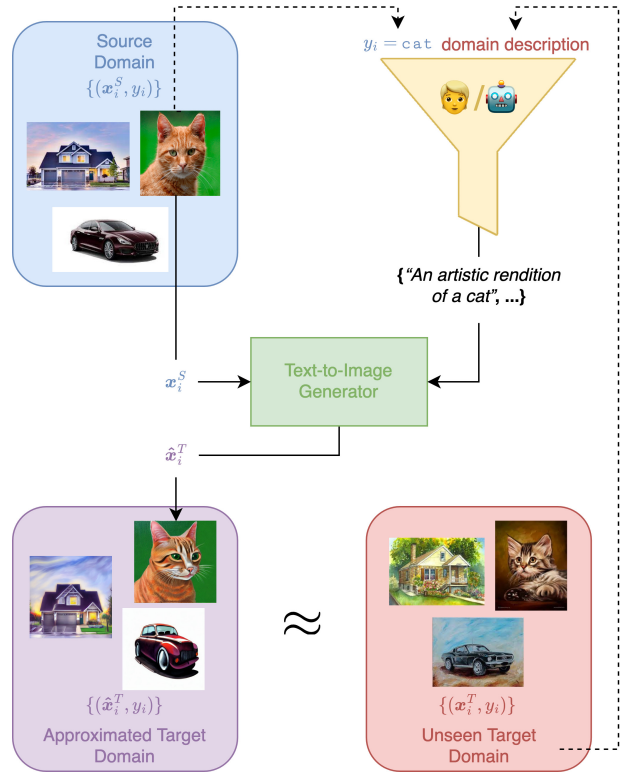


Figure 1. Using Text-to-Image (T2I) Generators to Manipulate Domain-Specific Features. A language user (which may be a human, a language model, or a collaboration between the two) is provided with a minimal description of the target domain and image class, and distills their prior knowledge into a natural language prompt, which is used by a T2I generator to synthetically transform an image from the source to the target domain. The generated data can be used to train more robust models. (Note that the prompt and generated images are sourced from our actual implementation.)

daylight have been observed to struggle when fed inputs captured at night [49]. Similarly, if the training set only contains photos of real-world objects, the performance degrades when those same objects are depicted through different media (e.g., illustrations, cartoons, or paintings) [29, 56].

To make classifiers robust to covariate-shift, researchers rely on assumptions about the test domains [47, 58]. While injecting invariances in the network architecture [18, 48, 64] or bounding their sensitivity to specific types of input perturbations [1, 50, 65] has achieved limited success, employing complex augmentation pipelines has been shown to be more effective and scalable [7, 21, 22, 40, 69, 71] when a single domain is accessible for training. These can both approximate the way the input features will be transformed in the test domains and perturb the training domain-specific features that do not generalise to unseen domains. One major drawback of this approach is that designing augmentation pipelines requires a trial-and-error process that can only be evaluated by measuring the accuracy on out-of-domain datasets. Indeed, most of the image manipulations produced are unrealistic [20, 22, 67], and their impact on classification performance can be difficult to understand.

As discussed in [26, 58], some types of augmentation primitives can be thought as approximating a controlled and targeted manipulation of the domain-specific environmental conditions in which the image was captured (e.g., illumination, point of view) without affecting the label-related features. In causal terminology, this means augmentations simulate an intervention on the environmental factors that are likely to change across domains, turning observational data (i.e., with no intentional manipulation of the environment) into interventional data (i.e., with intentional manipulation of the environment). Given that interventions on environmental conditions can often be described through natural language, Text-to-Image (T2I) generators (e.g., [5, 46]) can be used to interpret these descriptions and implement the desired image manipulation (see Fig. 1). The resulting synthetic samples approximate interventional data (which is typically expensive or even impossible to obtain) that can be leveraged to train more robust classifiers.

In this work, we formalize and instantiate a framework for interventional T2I augmentation, verifying that current technology is already sufficient to substantiate the promise of this approach. Our primary contributions are as follows:

- We show that T2I generators and natural-language prompts can be used to perform domain-specific visual interventions in the language-space rather than the pixel-space. This makes interventions more interpretable, transferable, and controllable, increasing the accessibility and effectiveness of interventional augmentations and enabling future “human-in-the-loop” [38] applications.
- We demonstrate that this approach can be used to (1) approximate the covariate-shift expected in test domains, producing state-of-the-art Single-Domain Generalization performance on widely-adopted benchmarks like PACS [29] and OfficeHome [56]; (2) weaken the reliance of classifiers on domain-specific

features (e.g., backgrounds, textures, and other spurious features); and (3) improve the performance of a state-of-the-art Multi-Domain Generalization technique (CIRL [35]) when few training domains are accessible by providing substitute synthetic training domains.

- We explore several possible instantiations of this framework, highlighting the role of prior domain knowledge and the resultant tradeoffs between involving humans “in-the-loop” and pursuing fully-automated approaches, discussing both the promise and limitations of current T2I generative models in a variety of use cases, and indicating actionable research directions to increase the scope and effectiveness of this framework.

2. Encoding Assumptions for Out-of-Domain Generalization

The problem of Out-Of-Domain Generalization Given a data distribution $P(\mathbf{x}, y) = P(y|\mathbf{x})P(\mathbf{x})$ where $\mathbf{x} \in \mathcal{X} \subset \mathbb{R}^d$, $y \in \mathcal{K} = \{1, 2, \dots, |\mathcal{K}|\}$, learning a classifier amounts to estimating $\hat{f}(\mathbf{x}) \approx P(y|\mathbf{x})$ (i.e., predicting the conditional distribution of the label y given a covariate \mathbf{x}) using a labelled training set $\mathcal{D}_{\text{train}} = \{(\mathbf{x}_i, y_i)\}_{i=1}^N$. Given the finite amount of data available in $\mathcal{D}_{\text{train}}$ and the high dimensionality of \mathcal{X} , the samples in $\mathcal{D}_{\text{train}}$ are not representative of the whole input space. This implies $\mathbf{x}_i \in \mathcal{X}_{\text{train}} \subset \mathcal{X}$ and therefore $\mathbf{x}_i \sim P_{\text{train}}(\mathbf{x})$. When deployed in the wild, the classifier will likely be exposed to inputs sampled from regions of the input space not represented in the training set, even when \mathcal{K} is the same. Formally, we are in presence of a specific type of distribution-shift called covariate-shift when, given $\mathbf{x}_i \sim P_{\text{test}}(\mathbf{x})$ whose support is $\mathcal{X}_{\text{test}} \subset \mathcal{X}$, it is assumed $\mathcal{X}_{\text{test}} \cap \mathcal{X}_{\text{train}} = \emptyset$ and $P_{\text{test}}(\mathbf{x}) \neq P_{\text{train}}(\mathbf{x})$ with unchanged $P(y|\mathbf{x})$. However, given at training time one can only access $\mathcal{D}_{\text{train}}$, a good approximation of $P(y|\mathbf{x})$ is only possible over $\mathcal{X}_{\text{train}}$, and equally good approximations $\hat{f}(\mathbf{x})$ on $\mathcal{X}_{\text{train}}$ can legitimately (at least theoretically) exhibit completely different behaviours on $\mathcal{X}_{\text{test}}$ (underspecification).

Being agnostic to the test domain is not an option Several theoretical frameworks have been developed to make the problem of out-of-domain generalization well-posed [26, 41, 58, 61]. At least in the image formation process, it is often assumed that pixel values \mathbf{x}_i are affected by the class label y_i and the specific configuration of some additional variables $\mathbf{c}_i \in \mathcal{C}$ (that we will call *environmental* or *contextual* variables) and that do not directly alter y_i . For instance, environmental variables could describe the illumination conditions, the position of the camera with respect of the object, the type of background, etc. It is also assumed

that it is possible to partition $\mathcal{C} = \bigcup_{j=1}^M \mathcal{C}^j, \mathcal{C}^k \cap \mathcal{C}^h = \emptyset, \forall k \neq h$ based on how similarly the environmental conditions impact \mathbf{x} . Starting from this setup, two main threads of research have been developed: Multi-Domain Generalization, MDG (i.e., m training environments are accessible, with $m > 1$) [55] and Single-Domain Generalization, SDG (i.e., $m = 1$) [40].

In MDG, it is assumed that observing data from different domains can help learn features that will generalise to previously unseen domains. However, a fine-grained control of the environmental conditions when sampling the dataset is not always feasible, and it might not always be possible to collect enough data from a sufficient number of distinct environments for these techniques to be effective. It is also unclear how numerous or diverse the training environments must be. Furthermore, such techniques exhibit widely different performance depending on which domains are chosen for training and test (e.g., see CIRL(3) in Tab. 7), especially when accessing only a finite (and often small) number of environments; and it has also been shown that it is not possible to learn optimal domain-invariant representations [47, 58] without further assumptions on the unseen domains.

Out-of-domain generalization is widely studied also in the context of SDG. In this setting, practitioners must encode their assumptions about the unseen domains, since invariances cannot be extracted based on the availability of different environments. While this encoding can be done through network design and bounding the sensitivity of the networks (see Appendix A for further discussion), we will proceed to focus on augmentation-based strategies.

Data augmentation strategies The traditional domain-agnostic data augmentation pipelines [6, 7, 11, 21, 22] contain prior knowledge about general desired invariances across domains through the composition of parametric image corruptions. For example, translations and shearing encode the belief that change of viewpoints should preserve the class label. Similarly, modifications in contrast and brightness encode the same belief with respect to changes in illumination and exposure conditions. Other augmentation strategies, drawing inspiration from Mixup [67], combine the features of multiple distinct images from the input (and corresponding labels) to improve generalization [39, 66, 72]. More advanced data augmentation techniques such as CIRL [35] and ACVC [7] manipulate the amplitude component of the image frequency spectrum of the Fourier transform, which presumes that it encodes environmental information. The purpose of these techniques is to simulate the effect of an intervention on the environmental conditions \mathbf{c}_i [26] and to leverage the intervened data to learn more robust representations.

Beyond the need for explicit implementations of image transformations, a clear disadvantage of this approach

is it requires careful tuning (often performed on splits of the test domains) and might not approximate the target domain environment very well. Partially addressing this issue, Adversarial Domain Augmentation (ADA) aims to synthesize domains through a generative model using adversarial training. The target is either to generate or augment images so that the results differ from the training distribution (e.g., [69, 71]) or to perturb the latent features to make classification harder (e.g., [25]). However, the results of this process belong to an unrealistic new domain that is neither guaranteed to be human-understandable nor generalise to all target domains.

3. Not Just Pretty Pictures: Generating Data From Language To Improve Robustness

Given the limitations of current augmentation techniques and the impressive performance of recent T2I generators [46], we suggest that these models may become a key tool to simulate environmental interventions in a human-understandable and customizable way.

Using T2I Generators to intervene on environmental variables Here, we consider how T2I Generators could transform samples from a source domain $\mathcal{C}^S = \mathcal{X}^S \times \mathcal{K}$ to a target domain $\mathcal{C}^T = \mathcal{X}^T \times \mathcal{K}$. Given an image $\mathbf{x}_i^S \in \mathcal{X}^S$ of class y_i from domain \mathcal{C}^S , let the token sequence $\mathbf{z}_i^S = (w_1, \dots, w_N)$ be a natural language description of \mathbf{x}_i^S where all $w_j \in \mathcal{V}_G$ for vocabulary \mathcal{V}_G of T2I generator G , allowing \mathbf{z}_i^S to serve as an image-generation prompt. For example, if \mathbf{x}_i^S is a painting of a cat (i.e., $y_i = \text{cat}, S = \text{painting}$), \mathbf{z}_i^S could be “a painting of a cat”, “napping kitten, watercolor on canvas, 2022”, etc. Our goal is to use T2I generators to translate an image \mathbf{x}_i^S to target domain \mathcal{X}^T , producing $\hat{\mathbf{x}}_i^T$ that preserves the original class y_i , but simulates the effect of the environmental conditions of \mathcal{X}^T by conditioning the generator on both \mathbf{x}_i^S and \mathbf{z}_i^T .¹ In the context of the previous example, we may define the target domain T as `cartoon`, in which case the task is to translate cat painting \mathbf{x}_i^S to cat cartoon $\hat{\mathbf{x}}_i^T$ using prompt \mathbf{z}_i^T (e.g., “a cartoon of a cat”, “kitten vector illustration”, etc.). If the generator is successful, it produces a sample $\hat{\mathbf{x}}_i^T \in \hat{\mathcal{X}}^T$, where $\hat{\mathcal{X}}^T \approx \mathcal{X}^T$. Finally, the set of synthetic pairs $\hat{\mathcal{C}}^T = \{(\hat{\mathbf{x}}_i^T, y_i)\}$ can be used to train a classifier together with \mathcal{C}^S .

Describing The Desired Intervention Let us now further detail how to produce the prompts \mathbf{z}_i^T . Notably, current neural language models can be highly sensitive to small differences in prompts that are not generally meaningful to humans [37, 45, 59]; and in our experiments, we observe T2I

¹We note that natural language descriptions are only required for the target domain \mathcal{C}^T , not \mathcal{C}^S ; \mathbf{z}_i^S is not used in this process.

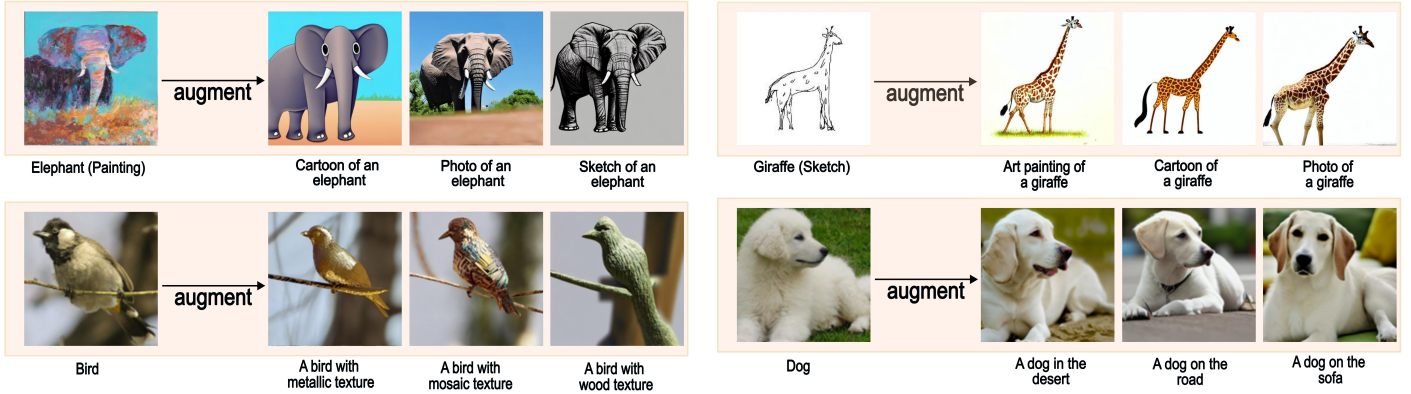


Figure 2. Interventional samples manipulated by Stable Diffusion. For each group of four images, the first left image is the original image, and the rest three images are augmented samples with text prompts indicated.

generators to be similarly sensitive. Therefore, it is important to find prompts that lead to high-quality results. In this work, we explore a few different prompting mechanisms, leveraging different sources of prior knowledge (cf. Fig. 1):

- **Minimal (M):** prompts including only the domain label, class label, and function words (like articles or prepositions) as necessary to make the prompt grammatically correct, like “a domain of a(n) class” (e.g., “a sketch of an elephant”).
- **Domain expert (H):** a collection of 1-8 simple “hand-crafted” prompts per image domain (e.g., “an ink pen sketch of a(n) class”), authored by a human domain expert given only the domain descriptions provided by the respective benchmarks without looking at any samples from the target domain.
- **Language enhancement (LE):** following [19], we use the T5 language model [43] fine-tuned on Common-Gen [31]² to generate 1-8 prompts using only the domain and class labels as inputs. Two strategies, Conservative (LE_C) and Moderate (LE_M), are used: the former deterministically generates high-probability outputs, whereas the latter induces more diversity using randomly sampled outputs with relatively high probability (see Appendix C for more information about LE ; for reference, in the above example, LE_C generates “sketch of an elephant in a zoo”, and LE_M generates “illustration of a wild elephant sketched on canvas”).

(For a complete list of image-generation prompts used in experiments, see Appendix I.)

Why using natural-language to describe interventions?

Using natural language prompts to generate interventions presents several advantages:

- **Interpretability:** Any fluent speaker of a language can easily interpret natural language prompts.
- **Transferability:** Natural language prompts describing a target domain are not specific to a particular pre-trained model, neural architecture, or source domain.
- **Controllability:** Natural language prompts can be modified ad-hoc based on human (or automated) feedback regarding generated images, model behavior, or the prompts themselves.

Additionally, natural language can easily summarise a wide variety of environmental conditions with only a few words. This makes it easy to specify environmental conditions using language (e.g., modifying the weather conditions described in a sentence), where it may be extremely difficult to produce such conditions in images using hand-crafted algorithms (e.g., turning an image of a sunny day into a realistic rainy one).

From Words To Pixels through T2I Generators

For this component of the framework, we mainly experiment with Stable Diffusion [46] (SD) pre-trained on LAION-Aesthetics [51] (which is a subset of the broader web-scraped text-image pairs dataset LAION-5B dataset [52] with high aesthetic scores), enabling us to transform an input \mathbf{x}_i^S into $\hat{\mathbf{x}}_i^T$ based on a prompt \mathbf{z}_i^T . It uses a Latent Diffusion Model (LDM) to gradually denoise normally distributed variables in latent space conditioning on both text prompt and original image through a reverse Markov chain process. We also report the results of some experiments with VQGAN-CLIP [5] in Appendix E. The synthetic data $\hat{\mathcal{C}}^T$, together with \mathcal{C}^S , can be used in many different ways. With no presumption of exhaustiveness, we showcase some relevant use cases (Fig. 2): aiding single-domain generalization (Sec. 3.1), weakening the reliance on spurious features (Sec. 3.2) and aiding a state-of-the-art Multi-Domain Generalization technique (CIRL [35]) when few training

²https://huggingface.co/mrm8488/t5-base-finetuned-common_gen

domains are available (Sec. 3.3).

3.1. Approximating Target Domains: Single-Domain Generalization

Given source domain \mathcal{C}^S that is accessible at training time, the goal of SDG is to achieve high performance on a set of target domains \mathcal{C}^{T_j} . The generator uses \mathcal{C}^S and $\mathbf{z}_i^{T_j}$ to generate $\hat{\mathcal{C}}^{T_j} \approx \mathcal{C}^{T_j}$. In this case, we treat the synthetic data as an augmentation for standard cross-entropy training, though more sophisticated usage of the synthetic data is also possible (see Sec. 3.3).

Datasets and Baselines We consider two standard benchmarks: (1) **PACS** [29] contains 9,991 images of four domains `art painting`, `cartoon`, `sketch`, and `photo`. (2) **Office-Home** [56] contains 15,500 images of four domains `Art`, `Clipart`, `Product`, and `Real World`. We train our models on one domain at a time and report the average test accuracy on the other three unseen domains. Besides reporting the Expected Risk Minimization (ERM) baseline trained with standard cross-entropy minimization, we examine a range of data augmentation methods from different categories. We compare methods including AugMix [21], RandAugment [6], CutOut [11], PixMix [22] that are developed for the general purpose of improving model robustness, as well as ACVC [7], which is developed specifically for SDG and achieves the state-of-the-art performance. We also compare with interpolation-based methods MixUp [67] and CutMix [66] as well as L2D [60], MEADA [69], and RSC [25] as the representative state-of-the-art ADA methods. Finally, we compare with SN [65] and SRN [50], which reduce perturbation sensitivity. To generate our dataset, we use the following prompting strategies: **M**, **H**, **LE_C**, and **LE_M**. The actual prompts of our method (OURS) are specified in Appendix I.

SDG Performance As shown in Tab. 1 and Tab. 2 our method achieves the highest performance across all the target domains regardless of the source domain chosen. Specifically, **OURS(H)** outperforms the previous SOTA SDG method ACVC and L2D by a considerable margin of **12.59%** and **14.96%** in PACS as well as **8.36%** and **10.09%** in OfficeHome taking the average over all target domains. Moreover, we observe that for settings where the other baseline methods fail to obtain significant improvement over ERM, such as from `art painting` to `cartoon` in PACS and `Clipart` to `Product` in OfficeHome (as shown in full per-test domain result Tab. 8 and Tab. 9 in Appendix B), our method still achieves a **17.45%** and **4.47%** improvement respectively. This shows that the

Table 1. Single Domain Generalization PACS result with ResNet-18. Columns are source domains; accuracies are the average test accuracy of three remaining target domains when training using the indicated source domain (best accuracies are in bold).

	Art	Photo	Sketch	Cartoon	Average
ERM	65.27	39.0	49.1	71.65	56.26
MixUp	56.3	35.22	39.07	62.71	48.33
CutMix	60.11	37.04	39.28	65.51	50.48
AugMix	64.85	40.05	57.59	73.19	58.92
RandAugment	68.81	44.24	58.2	72.9	61.04
CutOut	64.2	41.85	48.82	70.56	56.36
RSC	67.33	40.35	53.6	72.18	58.37
SN	67.17	46.44	36.96	60.1	52.67
SRN	67.68	45.7	38.83	62.52	53.68
MEADA	66.35	40.17	46.42	70.73	55.92
L2D	70.25	43.96	53.84	74.41	60.62
PixMix	64.19	40.37	51.61	75.08	57.81
ACVC	68.35	49.79	58.96	74.86	62.99
OURS(M)	79.86	65.22	70.37	76.38	72.96
OURS(H)	78.49	71.46	75.28	77.09	75.58
OURS(LE_C)	78.21	59.55	66.39	71.85	69.0
OURS(LE_M)	80.36	69.9	69.63	75.94	73.96

Table 2. Single Domain Generalization OfficeHome Result with ResNet-18, reported following the same practice as Tab. 1.

	Art	Clipart	Product	Real	Average
ERM	56.03	54.59	50.47	59.1	55.05
MixUp	51.33	43.8	42.72	53.24	47.77
CutMix	50.93	48.06	41.96	54.42	48.84
AugMix	55.99	55.51	52.72	59.22	55.86
RandAugment	57.98	56.54	53.22	61.13	57.22
CutOut	54.89	52.89	48.97	58.28	53.76
RSC	53.72	51.56	48.74	58.96	53.25
SN	40.79	39.1	36.56	50.32	41.69
SRN	40.11	38.78	37.55	49.99	41.61
MEADA	56.74	54.16	50.46	59.06	55.11
L2D	52.09	47.91	48.81	57.51	51.58
PixMix	54.7	53.34	50.47	59.05	54.39
ACVC	54.2	51.44	49.58	57.31	53.13
OURS(M)	62.86	60.71	57.11	62.9	60.9
OURS(H)	63.97	61.9	56.68	64.12	61.67
OURS(LE_C)	61.77	60.24	56.05	61.47	59.88
OURS(LE_M)	60.85	59.9	53.62	60.62	58.75

precise language-driven manipulations of our method enables generalization to more difficult cases, whereas hand-crafted manipulations can fail to bridge the distribution gap.

Untargeted SDG Performance Leveraging synthetic samples from additional domains can be beneficial also when the target test domain is unknown. To show this, instead of generating augmented samples for the three test domains of PACS and OfficeHome as we did in our previ-

Table 3. Effect of accessing target domain information on PACS and Officehome SDG result

PACS	Art	Photo	Sketch	Cartoon	Average
ERM	65.27	39.0	49.1	71.65	56.26
OURS(H/target)	78.49	71.46	75.28	77.09	75.58
OURS(H/untarget)	80.31	69.1	68.6	78.28	74.07
Officehome	Art	Clipart	Product	Real	Average
ERM	56.03	54.59	50.47	59.1	55.05
OURS(H/target)	63.97	61.9	56.68	64.12	61.67
OURS(H/untarget)	61.12	59.31	54.28	61.12	58.96

ous experiment, we now only generate samples in two domains, excluding the target test domain on which we measure the accuracy. In Tab. 3, we report the average accuracy on the left-out domains (i.e., we train three models for each source domain, one for each target domain). As it can be seen, preventing access to synthesized target domain samples gives rise to 1.51% and 2.71% drop of **OURS(H)** performance for PACS and OfficeHome respectively. Notably, in PACS, the 6.68% drop from `sketch` domain contributes the most to the overall lower performance; whereas in the `art painting` and `cartoon` domains, since the target domain shares common features with the synthetic domains, the performance is less affected. In Officehome, the drop in overall performance comes evenly from all settings. Thus, we conclude that models generalize best when they are able to access synthesized target-domain images, but explicitly generating the target domain is not necessary to achieve improved performance. We can use a smaller set of representative target domains to generalize to a wider range of unknown target domains as long as common features among them exist. In Tab. 10, we report the per-test domain performance for completeness.

3.2. Weakening The Reliance on Spurious Features

Neural classifiers trained via ERM are known to overly rely on spurious features. This makes them brittle in case the spurious correlation does not hold in the test domain too. We consider two standard benchmarks (for background [63] and texture [14] biases) and our own dataset to measure the reliance on simple but discriminative spurious features [53]. We hand-craft **(H)** the prompts \mathbf{z}_i^T to intentionally perturb these spurious features in the synthesized domain $\hat{\mathcal{C}}^T$ (prompts in Appendix I) and compare the performance with respect to metrics measuring the reliance on these features for models trained with standard cross-entropy training only on \mathcal{C}^S (ERM) and on both \mathcal{C}^S and $\hat{\mathcal{C}}^T$ (OURS)³.

³For a comparison with all the baselines and a thorough discussion about their varying effectiveness as well as metric calculation for each type of spurious feature, see Appendix B.3

Table 4. ImageNet-9: Gap (%) measures background reliance.

	I.I.D. Test	Mixed Rand	Mixed Same	Gap (↓)
ERM	95.16	73.54	86.02	12.48
OURS(H)	95.80	78.06	86.32	8.26

Table 5. Texture: Texture Bias (%) measures reliance on texture.

	I.I.D. Test	Random	Texture Bias (↓)
ERM	81.75	18.77	72.45
OURS(H)	88.13	26.33	64.17

Table 6. CelebA-sub: Gap(%) measures demographic reliance

	I.I.D. Test	Flip	Random	RandGap (↓)	FlipGap (↓)
ERM	99.44	77.16	88.48	10.96	22.28
OURS(H)	99.36	84.12	91.78	7.58	15.24

Background Bias We use the Original split of the **ImageNet-9** dataset from the Background Challenge [62] to train our models. As they suggest, we measure the **Gap** (↓) between the accuracies on images with the backgrounds manipulated using those from other images with the same class (Mixed same) or other classes at random (Mixed rand). From Tab. 4, we can see our method can significantly reduce this gap by **4.22%**.

Texture Bias We leverage the **Cue-Conflict Stimuli** dataset [14], which intentionally perturbs the images of a specific class with the texture patterns of another class. To train our models, we generate a training set by sampling from ImageNet-1K [10] the appropriate classes that represent the 16 classes of the benchmark. We then measure the reliance on texture using the **Texture Bias** (↓) as defined in [14]. From Tab. 5, our method reduces the Texture Bias by **8.28%**.

Demographic Bias We also perform an experiment where we create a subset of **CelebA** [34] to induce a controlled spurious correlation between the *Gender* and *Hair Colour*. The aim is to predict the *Gender*. In the training set, *Gender = Female* always co-occurs with *Hair Colour = Blonde*, while *Gender = Male* always co-occurs with *Hair Colour ≠ Blonde*. In the test set, we either invert the correlation (`flip`) or randomise (`random`) the co-occurrence of the two variables. The reliance on the spurious correlation is measured by **RandGap** (↓) and **FlipGap** (↓), which are the test accuracy difference of I.I.D and `random` or `flip` respectively. As shown in Tab. 6, we achieve **3.38%** and **7.04%** improvement against ERM on these two metrics.

Table 7. MDG result on PACS with (M/D) interventional data.

	Art	Photo	Sketch	Cartoon	Average
CIRL(1→3)	77.02	93.59	78.26	73.28	80.54
CIRL(1→4)	79.85	94.13	80.0	78.5	83.12
CIRL(2)	80.65	94.51	72.89	72.86	80.23
CIRL(2→3)	84.39	95.85	80.86	82.78	85.97
CIRL(2→4)	85.01	96.01	81.28	82.75	86.26
ERM(3)	80.01	96.28	73.86	76.28	81.61
CIRL(3)	85.35	95.93	82.69	80.89	86.22

3.3. Making Multi-Domain-Generalization Models Work Better With Less Domains

An important requirement for MDG techniques to be beneficial is the possibility of accessing multiple diverse training domains. This increases the cost of collecting training data. In this section, we investigate whether using synthetic data can aid when fewer training domains are available. We leverage CIRL [35], a SOTA MDG technique that, under the assumption the amplitude of the Fourier transform of an image encodes its style, uses an interpolation in the amplitude of two samples from different domains to simulate an intervention. The embedding of the augmented sample is contrastively aligned to the embedding of the original sample, and an adversarial masking mechanism is used to better leverage the learned representation.

One Real Training Domain In the extreme case only a single training domain can be accessed, MDG techniques are often ill-posed and cannot be applied. In Tab. 7, we show it is possible to apply CIRL [35], a state-of-the-art MDG technique, when a single training domain of the PACS dataset is available. We do so by using the generated domains as additional training domains, either providing prompts for the other two non-test domains (**CIRL(1→3)**) or for all the domains (including the test one) (**CIRL(1→4)**). In the former case, **CIRL(1→3)** slightly underperforms with respect to ERM(3) (which accesses 3 training domains), and significantly outperforms all methods in Tab. 1. **CIRL(1→4)** produces a further improvement of **7.54%** against best performing OURS(H), which is only 3.1% lower with respect to CIRL accessing all training domains (CIRL(3)).

Two Real Training Domains In case only two training domains are accessible as a baseline, we train CIRL on all possible pairs of domains that are not the test domain and report the average performance on the test domain (CIRL(2) in Tab. 7). We enhance the two training domains adding a synthetic one that does not describe the test domain (**CIRL(2→3)**) or adding descriptions of the test domain too (**CIRL(2→4)**). We observe that providing only a single synthetic domain induces a **5.74%** improvement; and adding the descriptors of the test domain improves it further

to **6.03%**, making it competitive with respect to using CIRL on 3 real domains (CIRL(3)).

4. Discussion

Sources of prior knowledge Overall, the SDG experiments in Sec. 3.1 indicate that our approach is most consistently successful when experts are available to distill their domain knowledge into prompts (H). However, when no such expert is available, even minimal prompts (M) are sufficient to outperform all data augmentation baselines. Furthermore, the results of the moderate language enhancement experiment (**LE_M**) on PACS indicate that applying current language models to automatically generate prompts can lead to performance that is comparable to prompts authored by domain experts (even outperforming them on two of four target domains).

When averaged across all domains, the OfficeHome experiments also show that expert-handcrafted prompts (H) perform best among all our methods, and that each of our methods still outperform all baselines. However, in this case, both **LE** methods drop below the minimal prompting method (M) on all domains. These results indicate that there is a tradeoff between consistency and automation: perhaps unsurprisingly, blindly applying language models to generate prompts with only minimal information can sometimes lead to lackluster results, as we see for OfficeHome; but in other cases, a fully-automated pipeline is still relatively successful (as in PACS). There are various strategies that may be employed to improve the consistency of automated methods; we discuss one such approach in the following section.

Prompt interpretability enables human-in-the-loop debugging Specifying interventions with natural language makes it possible to easily interpret and control their impact, enabling us to iteratively improve the fidelity of generated images to the desired augmentation. For example, in our texture bias experiment in Sec. 3.2, we began with a small set of handcrafted prompts (observing a decrease in texture bias of **5.44%**), then gradually expanded it to cover a broader range of textures to further decrease texture bias by an additional **2.84%** (see Appendix I and Tab. 13). More generally, it is possible to “debug” augmentations by directly analyzing prompts and modifying them to better reflect the desired intervention (which is possible with zero exposure to the target domain, or before augmented images are even generated). For example, the top prompts generated by **LE_M** for OfficeHome’s art domain and computer class include “art on a computer”, “a man is working on a computer with a piece of art on it”, etc., indicating that **LE_M** generated prompts describing scenarios where both the class and domain label refer to individual objects in a visual scene. In Appendix D, we describe a

few simple steps that can automatically filter out many such prompts⁴, illustrating the flexibility of the natural-language augmentation interface.

How much can your generator do given what it knows?

A natural question is how much the success of the proposed method depends on the generator’s knowledge of the target domains. In case the generator could only generate data for which it has been provided large amounts of highly-curated labelled data, it would yield little or no benefits with respect to using the collected data directly. While high-quality generation and editing requires at least a partial knowledge of the target domain, full supervision is not required: Stable Diffusion trains on text-image pairs scraped from the web with minimal post-processing (weak supervision). This is significantly less expensive than manually providing class and domain labels (with the added effort of controlling the environmental conditions). We also observe the emergent disentanglement properties of Stable Diffusion can help relaxing the requirement of collecting large amounts of samples of all classes for all the considered domains when scraping the web. To support this argument, we perform two experiments (see Appendix F for image examples and an in-depth discussion of the experiment setup):

- **Can the generators combine learned concepts to produce novel images?** If the generators could only combine the learned concepts in ways that have been observed in the training set, they would be functionally equivalent to image retrieval systems. In contrast, we observe that generators produce samples composing the learned concepts in ways that are not represented in their training distribution. For a few examples, see Fig. 3, where we compare the results of generating images and retrieving images from the training set. Although the individual entities specified in the prompts are in the training set, we were unable to retrieve an image depicting the specific combination of entities and relations between them that was specified in the prompt.
- **Can we perform precise and localised manipulations based on the prompts to intervene on out-of-distribution data?** We show it is possible to perform these kinds of manipulations not only on data from their training distribution (Fig. 2 and Fig. 4), but also on out-of-distribution data they generate (Fig. 5).

Further Discussion We discuss whether using a generator that produces lower-quality images is still useful for

⁴However, as our LE experiments are explicitly intended to operate fully autonomously (i.e., with no human intervention or supervision), we do not carry out a full-scale “debugged” version of this experiment – all reported OfficeHome results are from the “buggy” prompts.

training classifiers in Appendix E, and whether using multiple augmentations per sample and domain continue to improve the performance in Appendix F. Finally, in Appendix G, we discuss the limits of methods that bound the sensitivity of the network with respect to \mathcal{L}_p -ball perturbations to aid in generalization.

5. Towards More Powerful Interventional Frameworks With Future Text-to-Image Generators

In the previous sections, we demonstrate that it is possible to use off-the-shelf T2I generators to simulate interventions on the environmental features of an image using language, and that doing so allows us to train more robust classifiers. As T2I generators continue to improve, we anticipate that this general approach will become increasingly effective. Below, we discuss a few possible avenues for future improvements and applications, and detail the limitations faced by our current instantiations.

Fully automated applications We examine a basic implementation of a fully-automated augmentation pipeline in the language enhancement (LE) experiments above Sec. 3.1, finding that it sometimes achieved performance on-par with or exceeding that of the expert-handcrafted prompts. However, this language model is optimized to generate simple sentences describing commonplace scenarios (see Appendix C), not image-generation prompts. Thus, it is possible that fine-tuning language models to generate prompts that are better optimized for downstream T2I generators may yield superior results to expert-handcrafted prompts in many scenarios, making this approach a promising direction for future work. Another approach to improve fully-automated prompting involves continuous prompt optimization (also known as “prompt tuning” or “soft prompting”). Recently, these methods have been shown to outperform human-interpretable prompts for a variety of natural-language [27, 30, 33, 36] and vision-and-language [13, 70] tasks. These methods are not directly applicable to domain generalization because they require labelled samples to learn continuous prompts; but we suggest that they may be a promising fully-automated approach to domain adaptation tasks⁵ where prompt interpretability is not necessary (cf. [27]).

Human-in-the-loop applications As discussed in Sec. 3, using natural language prompts for T2I generation makes our approach interpretable, transferable, and controllable, facilitating a variety of novel use cases. For example, consider a “human-in-the-loop” (HITL) application context,

⁵I.e., where an unlabeled sample of the target domain is available to facilitate learning of the contextual features of the target domain [16].

where humans are available to provide interactive feedback to a model. In the HITL *active learning* paradigm, human experts perform the role of “oracles” that a model may “query” to provide labels of highly uncertain or novel inputs [38]. In contrast, our approach implements the *interactive machine teaching* paradigm [44], which treats human collaborators as *teachers* that may provide interactive feedback to update the “curriculum”⁶ of images used to train a model. For example, a human collaborator may observe that a model tends to perform poorly in the context of a given target domain, or that generated images do not capture some important stylistic properties of the domain. In response, they may easily compose or revise image-generation prompts with explicit reference to important features of the target domain. Critically, our approach allows human teachers to directly update visual curricula using natural language, providing models with feedback in much the same terms as one would a human student. We believe that the intuitiveness and efficiency of this approach makes it a promising approach to domain generalization, shifting the burden of the problem from human domain knowledge to natural language and thus enabling human collaborators to interactively instruct models without prerequisite domain expertise.

In particular, we argue that this benefit is particularly salient in the context of test-driven software engineering practice. Rather than blindly assuming that the performance on application-independent benchmarks will transfer to application-specific cases, engineers need to extensively document (often through natural language) the potential use cases and test conditions. The ability to directly specify these criteria via natural-language augmentations, or even directly reuse the documentation to generate training data, could be invaluable for controlling, predicting, and understanding the behaviour of vision models in real-world applications.

Limitations and Future Research One of the limitations of our work is that, although the quality of the intervened images can be judged subjectively by a domain expert, we have been unable to find an “objective” quality metric (either requiring access to a sample of the test domain or not) that is correlated with generalization performance across all experimental settings. Such a metric, if available, would enable automatic adjustments of prompts, deletion of low-quality samples, etc. Another limitation of our instantiations is that generating a single image (or batch of such with the same source image) with Stable Diffusion takes us up to ten seconds on a single GPU, requiring us to pre-generate each synthetic training set (see Appendix E). While Stable

⁶Note that, in our case, a curriculum is defined in terms of the domains from which training examples are drawn, not the order in which they are presented (cf. [3]).

Diffusion represents a significant improvement over other recent T2I generators in terms of GPU requirements [46], augmenting large datasets can still be prohibitive, requiring large compute resources to be carried out in a reasonable amount of time. As we discuss in Appendix F, in some cases the generator might manipulate some of the features associated with the causal variable. This can limit the performance of the proposed methodology and suggests that mechanisms to allow tighter control of the features to be manipulated should be devised to further improve the effectiveness of this technique. Lastly, while web-scale pre-trained generators can combine known objects and concepts in novel ways and therefore allow approximating interventions, we observed them failing in augmenting samples that were significantly out of their training distribution (e.g., on histological data; see Fig. 7). Similar to the trend of using foundation models for fine-tuning on small datasets to achieve improvements over training from scratch on these datasets [4], future work should investigate whether it is possible to leverage pre-trained T2I generators in order to successfully manipulate strongly out-of-domain inputs.

6. Conclusion

In this work, we develop and instantiate a framework employing off-the-shelf T2I generators as language-driven interventional tools to improve the robustness of image classifiers. Through extensive experiments, we show that recent technology empowers this approach to achieve state-of-the-art Single-Domain Generalization performance, reduce reliance on spurious features, and aid Multi-Domain Generalization techniques when few training domains are available. We highlight that existing techniques encode assumptions about how models should generalise to unseen domains, and discuss how natural language makes it possible to express such assumptions in an interpretable, transferable, and controllable way, enabling us to leverage human knowledge to iteratively improve trained classifiers. Given the rapid progress in T2I generation and corresponding editing capabilities in recent years, we anticipate that interventional T2I augmentation methodologies like ours will become a key component for the development of more robust machine learning systems.

Acknowledgements

This research is supported in part by the UKRI grant: Turing AI Fellowship EP/W002981/1 and EPSRC/MURI grant: EP/N019474/1. We would like to thank the Royal Academy of Engineering. Francesco Pinto’s PhD is funded by the European Space Agency (ESA). This research is based upon work supported in part by U.S. DARPA AIDA Program No. FA8750-18-2-0014. The views and conclusions contained herein are those of the authors and should

not be interpreted as necessarily representing the official policies, either expressed or implied, of DARPA, or the U.S. Government. The U.S. Government is authorized to reproduce and distribute reprints for governmental purposes notwithstanding any copyright annotation therein. We would like to thank Pau De Jorge Aranda, Ameya Prabhu and Fabio Pizzati for their valuable feedback.

References

- [1] Martin Arjovsky, Léon Bottou, Ishaan Gulrajani, and David Lopez-Paz. Invariant risk minimization. *arXiv preprint arXiv:1907.02893*, 2019. [2](#)
- [2] Peter Bandi, Oscar Geessink, Quirine Manson, Marcorcy Van Dijk, Maschenka Balkenhol, Meyke Hermsen, Babak Ehteshami Bejnordi, Byungjae Lee, Kyunghyun Paeng, Aoxiao Zhong, et al. From detection of individual metastases to classification of lymph node status at the patient level: the camelyon17 challenge. *IEEE Transactions on Medical Imaging*, 2018. [22](#), [23](#)
- [3] Yoshua Bengio, Jérôme Louradour, Ronan Collobert, and Jason Weston. Curriculum learning. In *Proceedings of the 26th annual international conference on machine learning*, pages 41–48, 2009. [9](#)
- [4] Rishi Bommasani, Drew A Hudson, Ehsan Adeli, Russ Altman, Simran Arora, Sydney von Arx, Michael S Bernstein, Jeannette Bohg, Antoine Bosselut, Emma Brunskill, et al. On the opportunities and risks of foundation models. *arXiv preprint arXiv:2108.07258*, 2021. [9](#)
- [5] Katherine Crowson, Stella Biderman, Daniel Kornis, Dashiell Stander, Eric Hallahan, Louis Castricato, and Edward Raff. Vqgan-clip: Open domain image generation and editing with natural language guidance. In *European Conference on Computer Vision*, 2022. [2](#), [4](#), [19](#)
- [6] Ekin D Cubuk, Barret Zoph, Jonathon Shlens, and Quoc V Le. Randaugment: Practical automated data augmentation with a reduced search space. In *Proceedings of the IEEE/CVF conference on computer vision and pattern recognition workshops*, pages 702–703, 2020. [3](#), [5](#)
- [7] Ilke Cugu, Massimiliano Mancini, Yanbei Chen, and Zeynep Akata. Attention consistency on visual corruptions for single-source domain generalization. In *Proceedings of the IEEE/CVF Conference on Computer Vision and Pattern Recognition (CVPR) Workshops*, pages 4165–4174, June 2022. [2](#), [3](#), [5](#)
- [8] Etienne David, Simon Madec, Pouria Sadeghi-Tehran, Helge Aasen, Bangyou Zheng, Shouyang Liu, Norbert Kirchgessner, Goro Ishikawa, Koichi Nagasawa, Minhajul A Badhon, Curtis Pozniak, Benoit de Solan, Andreas Hund, Scott C. Chapman, Frederic Baret, Ian Stavness, and Wei Guo. Global wheat head detection (gwhd) dataset: a large and diverse dataset of high-resolution rgb-labelled images to develop and benchmark wheat head detection methods. *Plant Phenomics*, 2020, 2020. [23](#)
- [9] Etienne David, Mario Serouart, Daniel Smith, Simon Madec, Kaaviya Velumani, Shouyang Liu, Xu Wang, Francisco Pinto Espinosa, Shahameh Shafiee, Izzat S. A. Tahir, Hisashi Tsujimoto, Shuhei Nasuda, Bangyou Zheng, Norbert Kirchgessner, Helge Aasen, Andreas Hund, Pouria Sadeghi-Tehran, Koichi Nagasawa, Goro Ishikawa, Sebastien Dandrfosse, Alexis Carlier, Benoit Mercatoris, Ken Kuroki, Haozhou Wang, Masanori Ishii, Minhajul A. Badhon, Curtis Pozniak, David Shaner LeBauer, Morten Lilimo, Jesse Poland, Scott Chapman, Benoit de Solan, Frederic Baret, Ian Stavness, and Wei Guo. Global wheat head dataset 2021: an

- update to improve the benchmarking wheat head localization with more diversity, 2021. [23](#)
- [10] Jia Deng, Wei Dong, Richard Socher, Li-Jia Li, Kai Li, and Li Fei-Fei. Imagenet: A large-scale hierarchical image database. In *2009 IEEE conference on computer vision and pattern recognition*, pages 248–255. Ieee, 2009. [6](#), [19](#)
- [11] Terrance DeVries and Graham W Taylor. Improved regularization of convolutional neural networks with cutout. *arXiv preprint arXiv:1708.04552*, 2017. [3](#), [5](#)
- [12] Patrick Esser, Robin Rombach, and Bjorn Ommer. Taming transformers for high-resolution image synthesis. In *Proceedings of the IEEE/CVF conference on computer vision and pattern recognition*, pages 12873–12883, 2021. [19](#)
- [13] Rinon Gal, Yuval Alaluf, Yuval Atzmon, Or Patashnik, Amit H. Bermano, Gal Chechik, and Daniel Cohen-Or. An image is worth one word: Personalizing text-to-image generation using textual inversion, 2022. [8](#), [18](#)
- [14] Robert Geirhos, Patricia Rubisch, Claudio Michaelis, Matthias Bethge, Felix A Wichmann, and Wieland Brendel. Imagenet-trained cnns are biased towards texture; increasing shape bias improves accuracy and robustness. *arXiv preprint arXiv:1811.12231*, 2018. [6](#)
- [15] Robert Geirhos, Patricia Rubisch, Claudio Michaelis, Matthias Bethge, Felix A. Wichmann, and Wieland Brendel. Imagenet-trained cnns are biased towards texture; increasing shape bias improves accuracy and robustness. In *ICLR*, 2019. [15](#)
- [16] Muhammad Ghifary, David Balduzzi, W Bastiaan Kleijn, and Mengjie Zhang. Scatter component analysis: A unified framework for domain adaptation and domain generalization. *IEEE transactions on pattern analysis and machine intelligence*, 39(7):1414–1430, 2016. [8](#)
- [17] Ishaan Gulrajani and David Lopez-Paz. In search of lost domain generalization. *arXiv preprint arXiv:2007.01434*, 2020. [1](#)
- [18] You Hao, Qi Li, Hanlin Mo, He Zhang, and Hua Li. Ami-net: Convolution neural networks with affine moment invariants. *IEEE Signal Processing Letters*, 25(7):1064–1068, 2018. [2](#), [14](#)
- [19] Ruifei He, Shuyang Sun, Xin Yu, Chuhui Xue, Wenqing Zhang, Philip Torr, Song Bai, and Xiaojuan Qi. Is synthetic data from generative models ready for image recognition? *arXiv preprint arXiv:2210.07574*, 2022. [4](#), [18](#)
- [20] Dan Hendrycks, Steven Basart, Norman Mu, Saurav Kadavath, Frank Wang, Evan Dorundo, Rahul Desai, Tyler Zhu, Samyak Parajuli, Mike Guo, Dawn Song, Jacob Steinhardt, and Justin Gilmer. The many faces of robustness: A critical analysis of out-of-distribution generalization. *ICCV*, 2021. [2](#)
- [21] Dan Hendrycks, Norman Mu, Ekin D. Cubuk, Barret Zoph, Justin Gilmer, and Balaji Lakshminarayanan. AugMix: A simple data processing method to improve robustness and uncertainty. *Proceedings of the International Conference on Learning Representations (ICLR)*, 2020. [2](#), [3](#), [5](#)
- [22] Dan Hendrycks, Andy Zou, Mantas Mazeika, Leonard Tang, Bo Li, Dawn Song, and Jacob Steinhardt. Pixmix: Dreamlike pictures comprehensively improve safety measures. *CVPR*, 2022. [2](#), [3](#), [5](#)
- [23] Amir Hertz, Ron Mokady, Jay Tenenbaum, Kfir Aberman, Yael Pritch, and Daniel Cohen-Or. Prompt-to-prompt image editing with cross attention control. *arXiv preprint arXiv:2208.01626*, 2022. [22](#)
- [24] Martin Heusel, Hubert Ramsauer, Thomas Unterthiner, Bernhard Nessler, and Sepp Hochreiter. Gans trained by a two time-scale update rule converge to a local nash equilibrium. In I. Guyon, U. Von Luxburg, S. Bengio, H. Wallach, R. Fergus, S. Vishwanathan, and R. Garnett, editors, *Advances in Neural Information Processing Systems*, volume 30. Curran Associates, Inc., 2017. [14](#)
- [25] Zeyi Huang, Haohan Wang, Eric P. Xing, and Dong Huang. Self-challenging improves cross-domain generalization. In *ECCV*, 2020. [3](#), [5](#)
- [26] Maximilian Ilse, Jakob M Tomczak, and Patrick Forré. Selecting data augmentation for simulating interventions. In Marina Meila and Tong Zhang, editors, *Proceedings of the 38th International Conference on Machine Learning*, volume 139 of *Proceedings of Machine Learning Research*, pages 4555–4562. PMLR, 18–24 Jul 2021. [2](#), [3](#), [14](#)
- [27] Daniel Khashabi, Xinxin Lyu, Sewon Min, Lianhui Qin, Kyle Richardson, Sean Welleck, Hannaneh Hajishirzi, Tushar Khot, Ashish Sabharwal, Sameer Singh, and Yejin Choi. Prompt waywardness: The curious case of discretized interpretation of continuous prompts. In *Proceedings of the 2022 Conference of the North American Chapter of the Association for Computational Linguistics: Human Language Technologies*, pages 3631–3643, Seattle, United States, July 2022. Association for Computational Linguistics. [8](#), [18](#)
- [28] Y. Lecun, L. Bottou, Y. Bengio, and P. Haffner. Gradient-based learning applied to document recognition. *Proceedings of the IEEE*, 86(11):2278–2324, 1998. [14](#)
- [29] Da Li, Yongxin Yang, Yi-Zhe Song, and Timothy Hospedales. Deeper, broader and artier domain generalization. In *The International Conference on Computer Vision (ICCV 2017)*, pages 5543–5551, 2017. [1](#), [2](#), [5](#)
- [30] Xiang Lisa Li and Percy Liang. Prefix-tuning: Optimizing continuous prompts for generation. In *Proceedings of the 59th Annual Meeting of the Association for Computational Linguistics and the 11th International Joint Conference on Natural Language Processing (Volume 1: Long Papers)*, pages 4582–4597, Online, Aug. 2021. Association for Computational Linguistics. [8](#)
- [31] Bill Yuchen Lin, Wangchunshu Zhou, Ming Shen, Pei Zhou, Chandra Bhagavatula, Yejin Choi, and Xiang Ren. CommonGen: A constrained text generation challenge for generative commonsense reasoning. In *Findings of the Association for Computational Linguistics: EMNLP 2020*, pages 1823–1840, Online, Nov. 2020. Association for Computational Linguistics. [4](#), [18](#)
- [32] Jeremiah Zhe Liu, Zi Lin, Shreyas Padhy, Dustin Tran, Tania Bedrax-Weiss, and Balaji Lakshminarayanan. Simple and principled uncertainty estimation with deterministic deep learning via distance awareness. *NeurIPS*, 2020. [23](#)
- [33] Pengfei Liu, Weizhe Yuan, Jinlan Fu, Zhengbao Jiang, Hiroaki Hayashi, and Graham Neubig. Pre-train, prompt, and predict: A systematic survey of prompting methods in nat-

- ural language processing. *arXiv preprint arXiv:2107.13586*, 2021. [8](#)
- [34] Ziwei Liu, Ping Luo, Xiaogang Wang, and Xiaoou Tang. Deep learning face attributes in the wild. In *Proceedings of International Conference on Computer Vision (ICCV)*, December 2015. [6](#)
- [35] Fangrui Lv, Jian Liang, Shuang Li, Bin Zang, Chi Harold Liu, Ziteng Wang, and Di Liu. Causality inspired representation learning for domain generalization. In *Proceedings of the IEEE/CVF Conference on Computer Vision and Pattern Recognition*, pages 8046–8056, 2022. [2](#), [3](#), [4](#), [7](#)
- [36] Sewon Min, Mike Lewis, Hannaneh Hajishirzi, and Luke Zettlemoyer. Noisy channel language model prompting for few-shot text classification. In *Proceedings of the 60th Annual Meeting of the Association for Computational Linguistics (Volume 1: Long Papers)*, pages 5316–5330, Dublin, Ireland, May 2022. Association for Computational Linguistics. [8](#)
- [37] Milad Moradi and Matthias Samwald. Evaluating the robustness of neural language models to input perturbations. *arXiv preprint arXiv:2108.12237*, 2021. [3](#)
- [38] Eduardo Mosqueira-Rey, Elena Hernández-Pereira, David Alonso-Ríos, José Bobes-Bascarán, and Ángel Fernández-Leal. Human-in-the-loop machine learning: A state of the art. *Artificial Intelligence Review*, pages 1–50, 2022. [2](#), [9](#)
- [39] Francesco Pinto, Harry Yang, Ser-Nam Lim, Philip H. S. Torr, and Puneet K. Dokania. Regmixup: Mixup as a regularizer can surprisingly improve accuracy and out distribution robustness, 2022. [3](#)
- [40] Fengchun Qiao, Long Zhao, and Xi Peng. Learning to learn single domain generalization. In *IEEE Conference on Computer Vision and Pattern Recognition (CVPR)*, pages 12556–12565, 2020. [2](#), [3](#)
- [41] Joaquin Quionero-Candela, Masashi Sugiyama, Anton Schwaighofer, and Neil D. Lawrence. *Dataset Shift in Machine Learning*. The MIT Press, 2009. [1](#), [2](#)
- [42] Alec Radford, Jong Wook Kim, Chris Hallacy, Aditya Ramesh, Gabriel Goh, Sandhini Agarwal, Girish Sastry, Amanda Askell, Pamela Mishkin, Jack Clark, Gretchen Krueger, and Ilya Sutskever. Learning transferable visual models from natural language supervision, 2021. [19](#)
- [43] Colin Raffel, Noam Shazeer, Adam Roberts, Katherine Lee, Sharan Narang, Michael Matena, Yanqi Zhou, Wei Li, Peter J Liu, et al. Exploring the limits of transfer learning with a unified text-to-text transformer. *J. Mach. Learn. Res.*, 21(140):1–67, 2020. [4](#), [18](#)
- [44] Gonzalo Ramos, Christopher Meek, Patrice Simard, Jina Suh, and Soroush Ghorashi. Interactive machine teaching: a human-centered approach to building machine-learned models. *Human-Computer Interaction*, 35(5-6):413–451, 2020. [9](#)
- [45] Marco Tulio Ribeiro, Tongshuang Wu, Carlos Guestrin, and Sameer Singh. Beyond accuracy: Behavioral testing of nlp models with checklist. *arXiv preprint arXiv:2005.04118*, 2020. [3](#)
- [46] Robin Rombach, Andreas Blattmann, Dominik Lorenz, Patrick Esser, and Björn Ommer. High-resolution image synthesis with latent diffusion models, 2021. [2](#), [3](#), [4](#), [9](#)
- [47] Yangjun Ruan, Yann Dubois, and Chris J. Maddison. Optimal representations for covariate shift. In *International Conference on Learning Representations*, 2022. [2](#), [3](#)
- [48] Sara Sabour, Nicholas Frosst, and Geoffrey E. Hinton. Dynamic routing between capsules. In *Proceedings of the 31st International Conference on Neural Information Processing Systems, NIPS’17*, page 3859–3869, Red Hook, NY, USA, 2017. Curran Associates Inc. [2](#), [14](#)
- [49] Christos Sakaridis, Dengxin Dai, and Luc Van Gool. Map-guided curriculum domain adaptation and uncertainty-aware evaluation for semantic nighttime image segmentation. *IEEE Transactions on Pattern Analysis and Machine Intelligence*, 2020. [1](#)
- [50] Amartya Sanyal, Philip H. Torr, and Puneet K. Dokania. Stable rank normalization for improved generalization in neural networks and gans. In *International Conference on Learning Representations*, 2020. [2](#), [5](#), [14](#), [23](#)
- [51] Christoph Schuhmann, Romain Beaumont, Richard Vencu, Cade Gordon, Ross Wightman, Mehdi Cherti, Theo Coombes, Aarush Katta, Clayton Mullis, Mitchell Wortsman, et al. Laion-5b: An open large-scale dataset for training next generation image-text models. *arXiv preprint arXiv:2210.08402*, 2022. [4](#)
- [52] Christoph Schuhmann, Romain Beaumont, Richard Vencu, Cade Gordon, Ross Wightman, Mehdi Cherti, Theo Coombes, Aarush Katta, Clayton Mullis, Mitchell Wortsman, et al. Laion-5b: An open large-scale dataset for training next generation image-text models. *arXiv preprint arXiv:2210.08402*, 2022. [4](#)
- [53] Harshay Shah, Kaustav Tamuly, Aditi Raghunathan, Prateek Jain, and Praneeth Netrapalli. The pitfalls of simplicity bias in neural networks. *Advances in Neural Information Processing Systems*, 33:9573–9585, 2020. [6](#), [15](#)
- [54] J. Taylor, B. Earnshaw, B. Mabey, M. Victors, and J. Yosinski. Rrxr1: An image set for cellular morphological variation across many experimental batches. In *International Conference on Learning Representations (ICLR)*, 2019. [22](#), [23](#)
- [55] Antonio Torralba and Alexei A. Efros. Unbiased look at dataset bias. *CVPR 2011*, pages 1521–1528, 2011. [3](#)
- [56] Hemanth Venkateswara, Jose Eusebio, Shayok Chakraborty, and Sethuraman Panchanathan. Deep hashing network for unsupervised domain adaptation. In *Proceedings of the IEEE Conference on Computer Vision and Pattern Recognition*, pages 5018–5027, 2017. [1](#), [2](#), [5](#), [18](#)
- [57] Jindong Wang, Cuiling Lan, Chang Liu, Yidong Ouyang, Tao Qin, Wang Lu, Yiqiang Chen, Wenjun Zeng, and Philip Yu. Generalizing to unseen domains: A survey on domain generalization. *IEEE Transactions on Knowledge and Data Engineering*, 2022. [1](#)
- [58] Ruoyu Wang, Mingyang Yi, Zhitang Chen, and Shengyu Zhu. Out-of-distribution generalization with causal invariant transformations. In *Proceedings of the IEEE/CVF Conference on Computer Vision and Pattern Recognition*, pages 375–385, 2022. [2](#), [3](#), [14](#)
- [59] Xuezhi Wang, Haohan Wang, and Diyi Yang. Measure and improve robustness in nlp models: A survey. *arXiv preprint arXiv:2112.08313*, 2021. [3](#)

- [60] Zijian Wang, Yadan Luo, Ruihong Qiu, Zi Huang, and Mahsa Baktashmotlagh. Learning to diversify for single domain generalization. In *Proceedings of the IEEE/CVF International Conference on Computer Vision*, pages 834–843, 2021. 5
- [61] Zihao Wang and Victor Veitch. A unified causal view of domain invariant representation learning. In *ICML 2022: Workshop on Spurious Correlations, Invariance and Stability*, 2022. 2
- [62] Kai Xiao, Logan Engstrom, Andrew Ilyas, and Aleksander Madry. Noise or signal: The role of image backgrounds in object recognition. *ArXiv preprint arXiv:2006.09994*, 2020. 6
- [63] Kai Yuanqing Xiao, Logan Engstrom, Andrew Ilyas, and Aleksander Madry. Noise or signal: The role of image backgrounds in object recognition. In *International Conference on Learning Representations*, 2021. 6, 15
- [64] Wenju Xu, Guanghui Wang, Alan Sullivan, and Ziming Zhang. Towards learning affine-invariant representations via data-efficient cnns. In *2020 IEEE Winter Conference on Applications of Computer Vision (WACV)*, pages 893–902, 2020. 2, 14
- [65] Yuichi Yoshida and Takeru Miyato. Spectral norm regularization for improving the generalizability of deep learning, 2017. 2, 5, 14, 23
- [66] Sangdoon Yun, Dongyoon Han, Seong Joon Oh, Sanghyuk Chun, Junsuk Choe, and Youngjoon Yoo. Cutmix: Regularization strategy to train strong classifiers with localizable features. In *Proceedings of the IEEE/CVF international conference on computer vision*, pages 6023–6032, 2019. 3, 5
- [67] Hongyi Zhang, Moustapha Cisse, Yann N Dauphin, and David Lopez-Paz. mixup: Beyond empirical risk minimization. *arXiv preprint arXiv:1710.09412*, 2017. 2, 3, 5
- [68] Richard Zhang, Phillip Isola, Alexei A Efros, Eli Shechtman, and Oliver Wang. The unreasonable effectiveness of deep features as a perceptual metric. In *CVPR*, 2018. 14
- [69] Long Zhao, Ting Liu, Xi Peng, and Dimitris Metaxas. Maximum-entropy adversarial data augmentation for improved generalization and robustness. In *Advances in Neural Information Processing Systems (NeurIPS)*, 2020. 2, 3, 5
- [70] Kaiyang Zhou, Jingkang Yang, Chen Change Loy, and Ziwei Liu. Learning to prompt for vision-language models. *International Journal of Computer Vision*, 130(9):2337–2348, 2022. 8
- [71] Kaiyang Zhou, Yongxin Yang, Timothy Hospedales, and Tao Xiang. Learning to generate novel domains for domain generalization, 2020. 2, 3
- [72] Kaiyang Zhou, Yongxin Yang, Yu Qiao, and Tao Xiang. Domain generalization with mixstyle. *arXiv preprint arXiv:2104.02008*, 2021. 3
- [73] Jun-Yan Zhu, Taesung Park, Phillip Isola, and Alexei A Efros. Unpaired image-to-image translation using cycle-consistent adversarial networks. In *Computer Vision (ICCV), 2017 IEEE International Conference on*, 2017. 14

Appendix

A. Other ways to encode invariances or performing interventions

Model-based strategies In computer vision, the practice of enforcing inductive biases drawn from the knowledge of tridimensional [48] and bidimensional [18, 28, 64] geometry through architecture design has had a long history, but with the exception of CNNs [28], these attempts have had limited success and faced serious scalability issues. Other approaches have tried to bound the sensitivity of networks to perturbations in the Euclidean space [50, 65] and studying its association with improved generalization. However, the assumption Euclidean distances correlate with human perception has been largely dismissed by the literature [24, 68], therefore bounding the sensitivity to Euclidean space perturbations of a model does not guarantee robustness to natural covariate shift. As our experiments confirm, although these approaches attain improvements in some cases, they do not provide consistent improvements across all the benchmarks we consider.

Performing interventions More similar in spirit to our approach are [58] and [26], which discuss the usage of augmentations in order to simulate interventions on the non-causal variables. While [26] suggests a mechanism to select parametric hand-crafted augmentations that will likely affect mostly the environmental factors and not the causal factors, [58] uses CycleGANs [73] to produce augmentations that simulate the availability of the same image in the other known domains. While these papers propose frameworks to tackle Multi-Domain Generalization, the purpose of our work is to stimulate research in the direction of using the flexible language-driven editing capabilities of T2I generators to approximate interventions.

B. Experiment Implementation

B.1. General Setup

Due to the inference speed limitation of generative models, we pre-generate all the augmentation images. For each image in the training set, we randomly selected k text prompts from the templates (see Appendix I). In the Single Domain Generalization experiments, we choose $k = 3$ prompts for each image (i.e., one prompt from each target domain), whereas for the weakening spurious correlation experiments, we choose $k = 4$ prompts for each image to randomize the correlation between the causal and spurious features. Then for each prompt **one** intervened image will be generated by the generative model and saved as a corresponding augmented version of the original image. At

training time, for each training image in the batch, one of its augmented versions will be randomly selected from the k pre-generated intervened samples. The general augmentation pipeline is shown in Algorithm 1.

Algorithm 1 Augmentation Algorithm

Input: Source Domain $\mathcal{D}_{\text{train}} = \{(\mathbf{x}_i, y_i)\}_{i=1}^N$, Target Domain Prior Knowledge $\mathcal{P}(\mathcal{D}_{\text{test}})$, PromptingStrategy $\in [M, H, LE_C, LE_M, I]$. GenerativeModel $\in [\text{StableDiffusion}, \text{VQGAN-CLIP}]$. Model $f(\theta, \mathbf{x})$

Output: Trained $f(\cdot)$

Pre-generation Stage :

```
1: for  $(\mathbf{x}_i, y_i)$  in  $\mathcal{D}_{\text{train}}$  do
2:   # select k prompts for each original image
3:   Prompts = []
4:   for  $_$  in  $\text{range}(k)$  do
5:     Prompts.append(PromptingStrategy( $y_i, \mathcal{P}(\mathcal{D}_{\text{test}})$ ))
6:   end for
7:   # generate one sample for each prompt
8:    $[\hat{\mathbf{x}}_i] \leftarrow \text{GenerativeModel}(\text{Prompts}, \mathbf{x}_i)$ 
9:   Save augmented samples in  $\mathcal{S} = \{\mathbf{x}_i : [\hat{\mathbf{x}}_i]\}_{i=1}^N$ 
10: end for
```

Training Stage :

```
11: for Batch  $(\mathbf{x}_i, y_i)_{i=1}^m$  in  $\mathcal{D}_{\text{train}}$  do
12:    $(\mathbf{x}_i, \hat{\mathbf{x}}_i) \leftarrow \text{Concat}(\mathbf{x}_i, \text{RandomSelect}(\mathcal{S}[\mathbf{x}_i]))$ 
13:   Train with cross-entropy loss  $\mathcal{L}$ 
14:    $\theta_{t+1} = \theta_t - \eta \sum_{i=1}^m \nabla_{\theta} \mathcal{L}(f(x_i), y_i)$ 
15: end for
16: return  $f(\cdot)$ 
```

Overall, given a dataset with N training samples, the generated interventional data will have a size of $N \times k$, where k is usually 3 – 4 throughout our experiments. Observe, the number of generated samples is generally low (given N is often of a few thousands): our technique is sufficiently data-efficient (i.e., it produces significantly better generalization with few additional generated samples) because the prompting mechanism can intentionally target specific types of interventions to weaken the spurious features or approximate the target domain. We report a few statistics about the training, validation and test set sizes as well as the number of classes for each dataset in Tab. 22.

At each training epoch we evaluate the validation accuracy and use the checkpoint producing the best validation accuracy to measure the test accuracy. All the results reported are based on the mean of 5 independent runs, except the combined MDG method (i.e CIRL), for which we use one seed given the need of averaging over multiple choices of the real training sets. For all the experiment, we use ResNet-18 pre-trained on ImageNet as the backbone model.

B.2. Single Domain Generalization

We set up the experiment under the standard Single Domain Generalization paradigm. For **PACS** and **Office-Home**, we train a model for each single domain and evaluate it on the rest three unseen domains for test accuracy. In these two datasets, we generate **three** augmented samples each one of them corresponds to one target domain. For all the datasets, we use an image size of 224×224 . The full experiment results are shown in following Tab. 8 and Tab. 9.

B.3. Weaken Spurious Correlation

In the three considered cases, the reliance on the spurious correlation is measured as: (1) **ImageNet-9** (Background Bias): **Gap**, as defined in [63], is the difference between the accuracies measured on the test sets `mixed same` and `mixed rand`. (2) **CCS Dataset** (Texture Bias): **Texture Bias**, as defined in [15], is the number of correct texture classifications over sum of the true positive texture and shape classifications. In the test CCS dataset, each image is synthesized with a texture and subject from different classes (i.e texture: elephant, class: cat). The true positive texture classification is the percentage of cases in which the model predicts the texture label correctly, similarly, true positive shape classification is the percentage of correctly classified shape labels. (3) **CelebA-sub** (Demographic Bias): **RandGap** and **FlipGap** represent the accuracy gap between **I.I.D** distribution to `rand` and `flip` respectively. The purpose is to measure the reliance on the spurious feature both for the average case (i.e., randomizing the spurious correlation in the test set) and in the worst case (i.e., the test set flips the spurious correlation). For all the three dataset each original image sample will have **four** pre-generated augmented samples. The comparison with all the baselines is in Tab. 11, Tab. 12, and Tab. 13. We discuss these results in Appendix B.4.

Additional Reversed CelebA-sub Experiment In the demographic experiment, we also investigate a setting that swaps the role of class label among the *Gender* and *Hair Colour* variables: we now consider *Hair Colour* as the class label and *Gender* as the spurious variable. As shown in Tab. 14, although our method still outperforms all the considered baselines (e.g., it produces 20.78% and 10.06% improvement on **FlipGap** and **RandGap** respectively over ERM), the test accuracy on the Flip and Random splits are in general much lower than on the I.I.D. test set. We observe that while the *Hair Colour* is a relatively simple feature, the *Gender* features are distributed all over the face and exhibit a higher degree of variability. It seems like all the considered methods tend to overly rely on this complex feature (see the significant drop in accuracy we observe when

flipping the spurious correlation). This seems to contradict the belief that simple features are leveraged more [53]. Although we leave to future investigations this phenomenon, we observe that networks might pick other simple spurious features that correlate to *Gender* (e.g., the presence of makeup), which might partially explain the apparent contradiction.

B.4. Untargeted Domain Generalization: can you perturb the spurious domain-specific features blindly?

Knowing the spurious features is crucial to perturb them effectively Several domain-generalization techniques argue their methodology is effective because it perturbs spurious training domain-specific features in a way that is often agnostic to the target domains. The empirical results of Tab. 11, Tab. 12, and Tab. 13 suggest these techniques are particularly effective when the spurious feature is targeted by the considered technique. For instance, ACVC incorporates two augmentations that specifically preserve edges and shape and remove textures and colours, therefore we observe it to be 4.92% less biased towards texture with respect to **OURS(H)v2**. However, the same method performs significantly worse with respect to **OURS(H)v2** in the other benchmarks about weakening spurious correlations. Similarly, PixMix perturbs the image with fractals and class-specific textures and performs extremely well on the Texture Bias experiment, but even worse than ERM on the CelebA experiment in Tab. 12 and comparably on ImageNet-9 Tab. 11. L2D performs much better in Tab. 13 than Tab. 14, which is not particularly surprising considering that it applies a transformation that modifies the style (Texture and Colour), and therefore could potentially have little effect on the backgrounds or more complex combinations of features. SN and SRN achieve remarkably low Texture and Background Bias scores, but they also negatively affect the i.i.d. test accuracy, indicating that, although bounding the sensitivity of the networks to \mathcal{L}^p perturbations is effective in reducing the sensitivity to texture and background changes, it also hinders the ability to learn. A low sensitivity to such perturbations is nevertheless ineffective in Tab. 12.

Should you know all your test domains? Augmentation techniques can be effective because they approximate the target domains, perturb training-specific spurious features and learn invariances that generalize to the test domains, or a combination of the two. Intuitively, with a large enough set of augmentations that do not alter the label of the input image, it is possible to perturb all the spurious features and learn domain-invariant representations. However, it is possible that a minimal set of augmentations exists such that the learned representation generalizes across a wide range

Table 8. PACS result with ResNet-18

Source Domain	art			photo			sketch			cartoon		
Target Domain	photo	sketch	cartoon	art	sketch	cartoon	art	photo	cartoon	art	photo	sketch
ERM	96.24	53.3	63.27	66.08	30.74	29.19	37.98	47.12	60.24	68.07	85.64	67.57
MixUp	93.22	41.65	54.57	59.33	28.44	25.52	29.84	39.46	46.85	63.54	83.53	53.42
CutMix	93.75	47.46	57.36	60.52	33.65	22.22	28.55	37.37	50.0	64.8	83.59	58.2
AugMix	96.48	52.23	63.45	65.6	31.58	31.91	50.21	56.78	64.61	73.32	88.63	66.54
RandAugment	95.82	61.63	61.61	66.05	38.87	34.2	50.46	58.39	64.82	68.84	85.75	69.57
CutOut	96.04	52.39	61.31	64.24	36.83	30.71	36.88	49.25	58.95	66.39	82.88	67.5
RSC	94.49	56.57	66.02	67.24	33.69	28.02	45.64	51.58	61.98	68.57	84.78	68.71
SN	81.27	64.39	61.79	48.36	50.17	38.49	26.04	24.22	55.58	48.65	62.47	65.06
SRN	81.1	66.88	59.45	50.29	48.88	36.37	28.34	26.77	56.59	48.28	64.16	69.25
MEADA	95.4	54.23	65.97	63.94	33.84	30.01	33.94	41.78	60.63	66.72	84.11	67.13
L2D	94.41	61.25	68.11	65.12	39.56	32.86	44.04	52.04	63.7	72.98	86.45	70.05
PixMix	96.03	52.01	61.94	66.57	32.42	30.82	42.97	51.44	59.29	75.74	87.94	69.27
ACVC	95.23	59.41	64.2	67.78	47.64	37.67	53.38	58.47	64.18	74.32	86.69	70.12
OURS(M/G)	96.58	65.27	72.42	67.82	43.63	51.69	41.44	51.22	68.68	71.92	89.03	72.34
OURS(M/D)	96.84	71.97	80.97	71.13	61.26	66.69	56.68	81.03	74.75	75.98	90.11	70.75
OURS(H/D)	96.71	69.41	80.72	73.7	69.92	72.09	66.23	86.25	75.37	76.3	89.96	72.04
OURS(LE_C/D)	95.27	71.0	78.16	68.44	53.18	62.46	55.08	76.37	69.15	68.15	84.65	68.35
OURS(LE_M/D)	96.31	74.83	78.26	73.74	65.52	73.88	60.77	78.71	70.91	70.63	90.58	72.49

Table 9. Office-Home result with ResNet-18

Source Domain	Art			Clipart			Product			Real		
Target Domain	Clipart	Product	Real	Art	Product	Real	Art	Clipart	Real	Art	Clipart	Product
ERM	42.68	57.99	67.4	44.42	56.3	58.51	41.38	39.86	66.18	56.5	46.16	73.25
MixUp	36.94	53.61	63.42	32.18	46.81	47.2	33.23	32.34	58.41	51.11	39.39	68.01
CutMix	37.0	53.3	62.46	34.97	51.88	51.47	32.26	31.29	58.06	52.6	40.13	69.47
AugMix	43.16	57.36	67.45	44.55	57.66	59.44	43.62	43.32	67.2	56.42	47.49	72.28
RandAugment	46.31	59.91	67.69	44.83	59.31	60.25	41.6	46.37	66.55	57.68	50.57	73.39
CutOut	40.88	57.09	66.7	41.7	55.45	56.51	40.13	38.24	64.63	56.25	44.92	72.52
RSC	40.74	55.41	65.0	42.8	52.52	55.47	38.57	40.03	63.13	56.1	46.69	72.58
SN	34.89	38.23	49.3	27.12	41.69	43.14	22.02	34.77	46.47	42.76	44.44	60.24
SRN	34.26	37.47	48.65	26.88	41.21	42.93	23.52	34.36	48.55	42.85	44.03	59.75
MEADA	43.68	58.83	67.7	43.7	56.09	58.0	41.11	40.08	66.08	56.49	46.53	72.78
L2D	42.49	51.38	62.42	38.29	48.69	52.46	37.25	43.55	60.52	53.26	48.71	68.5
PixMix	41.95	56.44	65.7	42.79	56.04	56.45	42.12	41.0	64.6	57.59	47.23	71.49
ACVC	43.25	54.45	64.93	40.95	53.41	55.29	38.61	42.66	62.63	54.55	47.57	68.4
OURS(M/G)	47.41	64.44	71.94	48.92	65.27	67.13	48.4	44.34	70.84	59.27	49.81	73.67
OURS(M/D)	52.46	64.07	72.05	47.69	63.47	65.15	45.83	50.32	70.19	57.44	55.57	73.09
OURS(H/D)	52.33	66.53	73.03	47.03	66.01	66.0	46.08	49.32	69.94	58.25	56.17	75.15
OURS(LE_C/D)	51.04	63.59	70.65	47.04	62.99	64.79	45.79	48.55	69.29	56.73	52.93	72.47
OURS(LE_M/D)	50.4	62.25	69.91	46.08	63.43	64.0	43.2	46.11	66.95	56.57	51.84	71.48

of domains of interest. In our work, we choose to explicitly target either the test domains or the spurious features to perturb to reduce the complexity and variety of augmentations that need to be applied. This is a key advantage of our methodology: we do not encode the desired invariances in a set of pre-defined augmentations (as domain-agnostic tech-

niques do), which might not generalise in all the considered settings, but rather enable flexible specification of the desired invariances via prompts and generated images. An interesting open research question is how to select a minimal set of augmentations that allows one to obtain the same generalization performance.

Table 10. Effect of accessing target domain information on PACS and Officehome SDG result

PACS	art			photo			sketch			cartoon		
Target Domain	photo	sketch	cartoon	art	sketch	cartoon	art	photo	cartoon	art	photo	sketch
ERM	96.24	53.3	63.27	66.08	30.74	29.19	37.98	47.12	60.24	68.07	85.64	67.57
OURS(H/target)	96.71	69.41	80.72	73.7	69.92	72.09	66.23	86.25	75.37	76.3	89.96	72.04
OURS(H/untarget)	96.41	70.32	74.19	70.85	67.6	68.86	58.74	79.88	67.19	77.98	89.34	67.52

Officehome	Art			Clipart			Product			Real		
Target Domain	Clipart	Product	Real	Art	Product	Real	Art	Clipart	Real	Art	Clipart	Product
ERM	42.68	57.99	67.4	44.42	56.3	58.51	41.38	39.86	66.18	56.5	46.16	73.25
OURS(H/targeted)	52.33	66.53	73.03	47.03	66.01	66.0	46.08	49.32	69.94	58.25	56.17	75.15
OURS(H/untargeted)	48.0	64.09	71.26	49.28	64.81	63.85	45.16	48.16	69.52	56.45	53.08	73.82

Table 11. ImageNet-9 result with ResNet-18

	I.I.D. Test	Mixed Rand	Mixed Same	Gap (↓)
ERM	95.16	73.54	86.02	12.48
MixUp	94.62	67.63	83.91	16.28
CutMix	95.36	65.21	84.77	19.56
AugMix	95.16	74.73	87.72	12.99
RandAugment	96.69	78.20	90.44	12.25
CutOut	95.46	71.10	85.41	14.31
RSC	94.12	74.72	84.39	9.68
SN	77.78	62.33	71.35	9.01
SRN	77.58	60.26	70.18	9.93
MEADA	95.56	74.74	87.43	12.69
PixMix	97.04	79.76	91.96	12.20
ACVC	93.97	76.38	88.16	11.77
L2D	92.84	73.04	84.10	11.06
OURS(H/G)	95.95	74.42	85.88	11.46
OURS(H/D)	95.80	78.06	86.32	8.26

Table 12. CelebA-sub result with ResNet-18

	I.I.D. Test	Flip	Random	FlipGap (↓)	RandGap (↓)
ERM	99.44	77.16	88.48	22.28	11.32
MixUp	99.16	79.4	88.86	19.76	9.46
CutMix	99.24	74.82	86.92	24.42	12.1
AugMix	99.56	76.42	87.82	23.14	11.4
RandAugment	99.04	77.62	88.96	21.42	11.34
CutOut	99.48	78.24	89.72	21.24	11.48
RSC	99.52	81.7	91.8	17.82	10.1
SN	98.4	73.78	85.82	24.62	12.04
SRN	98.32	75.2	86.54	23.12	11.34
MEADA	99.48	77.24	89.08	22.24	11.84
ACVC	99.16	79.5	89.58	19.66	10.08
PixMix	99.32	76.62	88.34	22.7	11.72
L2D	99.12	81.96	90.96	17.16	9.0
OURS(H)	99.36	84.12	91.78	15.24	7.66

B.5. Hyperparameters

Training Hyperparameter For all the other baselines, we use the value as proposed in their original papers or official implementation. The training hyperparameters for setting is specified as shown in Tab. 15

Table 13. Texture result with ResNet-18

	I.I.D. Test	Random	Texture Bias (↓)
ERM	81.75	18.77	72.45
MixUp	77.36	19.23	71.69
CutMix	79.96	15.64	77.16
AugMix	82.2	20.08	72.42
RandAugment	83.09	18.9	72.2
SN	70.8	38.73	37.72
SRN	69.77	38.58	37.55
CutOut	81.85	17.81	74.19
RSC	79.9	20.48	71.11
MEADA	81.97	19.5	71.14
PixMix	80.91	26.86	64.64
ACVC	81.13	29.33	59.25
L2D	80.06	23.55	62.12
OURS(H)v1	87.37	25.39	67.01
OURS(H)v2	88.13	26.33	64.17

Table 14. CelebA-sub reversed result with ResNet-18

	I.I.D. Test	Flip	Random	FlipGap (↓)	RandGap (↓)
ERM	99.8	20.2	59.34	79.6	39.14
MixUp	99.68	20.74	60.2	78.94	39.46
CutMix	99.76	23.46	61.5	76.3	38.04
AugMix	99.76	19.12	59.46	80.64	40.34
RandAugment	99.88	22.86	61.0	77.02	38.14
CutOut	99.88	22.54	60.36	77.34	37.82
RSC	99.84	18.96	58.02	80.88	39.06
SN	99.12	27.72	62.82	71.4	35.1
SRN	99.4	25.3	62.14	74.1	36.84
MEADA	99.48	23.54	60.38	75.94	36.84
ACVC	99.8	21.62	60.54	78.18	38.92
PixMix	99.88	24.2	61.2	75.68	37.0
L2D	100.0	16.78	57.62	83.22	40.84
OURS(H)	99.64	40.82	69.9	58.82	29.08

Generator Hyperparameter For the two types of generative models, we use the hyperparameters for each dataset as shown in Tab. 16. Hyperparameters are tuned based on human judgement of few-shot image manipulation quality, without downstream task accuracy based evaluation. Un-

Table 15. Training Hyperparameters

	PACS	OfficeHome	ImageNet-9	Texture	CelebA-sub
Epoch	30	50	30	30	30
Batch size	64	64	64	64	64
Warmup Epoch	5	5	5	5	5
Warmup Type	sigmoid	sigmoid	sigmoid	sigmoid	sigmoid
Weight Decay	5e-4	5e-4	5e-4	5e-4	5e-4
Nesterov	True	True	True	True	True
Learning rate	1e-3	3e-3	1e-3	1e-3	1e-3
Scheduler	Step	Step	Step	Step	Step
Decay Step	27	45	27	27	27
Learning rate decay	0.1	0.3	0.1	0.1	0.1

specified hyperparameters are set to their default value.

C. Automated Prompting Methods

C.1. Language Enhancement

For our Language Enhancement (LE) experiments, we use a T5 [43] model that is pre-trained on both unsupervised language modeling of web text and supervised text-to-text language modeling tasks⁷, then fine-tuned on CommonGen⁸ [31], following [19]. (We will refer to this model as T5_{CG}.) CommonGen is a constrained-generation task whose objective is to generate a sentence describing a commonplace scenario that contains all words⁹ provided in an input word set. For example, given the words {dog, frisbee, catch, throw}, an acceptable output is “The dog catches the frisbee when the boy throws it.” [31] We always provide T5_{CG} with a text input containing only a domain label and class label; for example, given a PACS image with domain *sketch* and class *elephant*, we simply feed T5_{CG} “sketch elephant” as input.

Experimental Configurations We use two separate LE configurations, *conservative* (LE_C) and *moderate* (LE_M). LE_C is designed to generate consistent, high-probability outputs, and LE_M is built to balance prompt diversity with quality. For n number of prompts we will use to generate images, in LE_C, we simply use beam search decoding to generate prompts with $4n$ beams and select the top- n highest probability beams. In LE_M, we use a conjunction of top- k and top- p (nucleus) sampling, with $k = 50$ and $p = 0.95$, returning n sampled prompts. We experimented with other decoding configurations, but found that increasing prompt diversity (e.g., by increasing k , lowering p , or increasing

⁷Pre-trained model (not directly used in experiments): <https://huggingface.co/t5-base>

⁸Fine-tuned model used in experiments: https://huggingface.co/mrm8488/t5-base-finetuned-common_gen

⁹Synonyms and inflected forms are also allowed (e.g., given input “eat”, outputs containing “consume” or “eaten” are valid).

temperature) consistently came at the cost of prompt quality. We recommend that future work investigate the use of techniques such as CLIP filtering (cf. [19]) to remove low-quality image-generation prompts, which may enable a more favorable tradeoff between prompt diversity and quality.

C.2. Textual Inversion

We also experimented with few-shot domain adaptation using textual inversion [13], learning continuous input tokens specialized for each domain and image class by optimizing over 8 image samples from the target domain/class, then including the learned token in minimal generation prompts (e.g., “a <CLASS> in the style of S_* ”, for learned token S_*). A comparison of our best-performing variant of this method (denoted I) with our other prompting strategies is available in Tabs. 17 and 18, which show that it underperforms alternatives.

As discussed in Sec. 5, continuous prompt optimization techniques like textual inversion frequently perform better than interpretable, handcrafted prompts; so it is not unlikely that such techniques could still be a powerful tool in the context of our framework, given sufficient effort to tune them to the desired application context. However, prompt optimization approaches are less broadly applicable than the minimal, handcrafted, and language-enhancement strategies that we consider, as they require a sample of the target domain (making them only suitable for domain adaptation, not generalization) and are not human-interpretable (see [27]). Thus, we suggest that future work consider these tradeoffs before investing substantial effort into developing such approaches for interventional T2I augmentations.

D. Human-in-the-Loop Debugging

As discussed in Sec. 4, LE_M is prone to generating prompts that treat OfficeHome [56] domain labels as objects, not as visual domains or styles. Fortunately, the interpretability of natural-language prompts that makes it possi-

Table 16. Generator hyperparameters for each dataset

	PACS	OfficeHome	ImageNet-9	CelebA-sub	Texture
Stable Diffusion					
num_inference_step	80	80	50	50	50
strength	0.9	0.9	0.9	0.9	0.9
guidance_scale	7.5	7.5	7.5	7.5	7.5
VQGAN-CLIP					
max_iteration	100	100	100	100	100

Table 17. Prompting Strategy Comparison on PACS: Average (single-seed; for average across multiple seeds, see Tab. 1)

	art	photo	sketch	cartoon	Average
M	79.86	65.22	70.37	76.38	72.96
H	78.9	71.9	75.63	78.16	76.15
LE _C	78.21	59.55	66.39	71.85	69.0
LE _M	80.36	69.9	69.63	75.94	73.96
I	74.25	68.12	66.04	74.78	70.8

ble for us to diagnose this problem also enables us to filter out many such prompts. One approach is to map domain labels to the visual conditions they denote: for example, the `Product` label may be replaced with “white background”, `Real World` with “photograph”, etc. However, this solution requires some knowledge about test domains, which may not always be available. Alternatively, image-related keywords like “image”, “depict”, or “style” can be included in the input issued to T5_{CG} (see Appendix C.1), and outputs which do not place these additional terms in the same minimal noun phrase as the domain label can be removed (e.g., “an artistic depiction of a computer” or “a product image of a candle” would be kept, whereas “art depicted on a computer” or “a product and an image of a candle” would be excluded)¹⁰. While both of these strategies require limited human oversight to successfully “debug” prompts, more sophisticated fully-automated augmentation pipelines might learn to make such changes on their own, e.g., by integrating downstream image classifier accuracy as feedback to fine-tune prompt-generation models.

E. Do you need pretty pictures?

E.1. Using VQGAN-CLIP instead of Stable Diffusion

In our pipeline, we replace Stable Diffusion with VQGAN-CLIP [5] (G). Similarly to Stable Diffusion, VQGAN-CLIP allows to transform an input \mathbf{x}_i^S into $\hat{\mathbf{x}}_i^T$

¹⁰For clarity, T5_{CG} can replace input terms with inflected forms in generated prompts, e.g., allowing input terms “art” and “depict” to occur as “artistic” and “depiction” (respectively) in outputs (see Appendix C.1).

based on a prompt \mathbf{z}_i^T . VQGAN-CLIP utilizes the Contrastive Language–Image Pre-training (CLIP) [42] model to calculate the similarity between VQGAN [12] generated image and text prompt, then use the similarity score as a loss function to recursively optimize the latent representation until the generated image is close enough to target prompt. VQGAN-CLIP relies on ImageNet-1K [10] for training and the availability of CLIP (which is in turn trained on a private dataset of text-image pairs scraped from the web). We have observed VQGAN-CLIP produces qualitatively worse results with respect to Stable Diffusion, therefore in the main paper we report results only for the latter.

E.2. Computational Expense

The general statistics of computational expense of each type of generative model on a NVIDIA A40 GPU and generator with hyperparameters specified for OfficeHome experiment is shown in Tab. 19.

E.3. Effect of Image Quality

Pretty pictures are not always needed, but much appreciated. For how good modern Text-To-Image Generators can be, they can still produce unrealistic results or exhibit artifacts. Although VQGAN-CLIP often produces worse results than Stable Diffusion, in Tab. 8 and Tab. 9 we observe that using VQGAN-CLIP samples exhibits competitive performance with respect to Stable Diffusion. This suggests that for some forms of shift, it is not necessary for the generator to output well-formed images to induce improved performance: it is sufficient for it to reproduce some of the target domain features. For example, consider transform to cartoon domain in Appendix F (Fig. 6): although these images are unrealistic cartoons, they reproduce some of the features of cartoons such as the uniform colors, the presence of thick dark edges, etc. However, over-reliance on low-quality generated images makes the process less human-friendly, reducing the interpretability of the augmentations. We also observe that when the mapping between domains is particularly hard (e.g., in PACS, turning a Photo into a Sketch), the proposed technique can underperform with respect to other (e.g., (M/G) provides a 43.63 accuracy in the aforementioned setting, while ACVC provides 47.64 and

Table 18. Prompting Strategy Comparison on PACS: Detailed

Source Domain	art			photo			sketch			cartoon		
Target Domain	photo	sketch	cartoon	art	sketch	cartoon	art	photo	cartoon	art	photo	sketch
M	96.84	71.97	80.97	71.13	61.26	66.69	56.68	81.03	74.75	75.98	90.11	70.75
H	96.88	70.21	80.65	74.05	70.46	72.44	66.85	86.25	75.73	76.64	90.58	73.68
LE _C	95.27	71.0	78.16	68.44	53.18	62.46	55.08	76.37	69.15	68.15	84.65	68.35
LE _M	96.31	74.83	78.26	73.74	65.52	73.88	60.77	78.71	70.91	70.63	90.58	72.49
I	89.72	63.52	81.21	71.45	66.27	68.31	55.85	68.71	73.05	70.68	81.09	74.24

Table 19. Computational Expense of Image Manipulation

	Memory Usage(GB)	Computational Time(sec/sample)
VQGAN-CLIP	6.5	10
Stable Diffusion	11	15

Table 20. PACS SDG result with contrastive training

	Art	Photo	Sketch	Cartoon	Average
ERM	65.27	39.0	49.1	71.65	56.26
OURS(H/D/CE)	78.49	71.46	75.28	77.09	75.58
OURS(H/D/COS)	81.35	72.16	70.37	77.36	75.31
OURS(H/D/L2)	81.24	67.82	71.49	77.92	74.62

SN 50.17) as shown in (Tab. 8; see Appendix B). Additionally, for more fine-grained tasks like reducing the reliance on background features (Tab. 11; see Appendix B), the low quality images of VQGAN-CLIP produce a background reliance gap value of 11.46, which is slightly better than ERM and significantly worse than Stable Diffusion. Similarly, inverting the role of the label and the spurious feature in the CelebA experiment (where the class label is the hair colour and the spurious variable is the gender), the transformation between domains becomes harder and the performance of the proposed method degrades (Tab. 14; see Appendix B). Therefore, although producing high quality images is not always necessary, it is still useful to allow more nuanced and fine-grained control of the desired behaviour of the networks. Given that Stable Diffusion tends to produce better quality images, we prefer it when performing our analyses.

E.4. Manipulating only the environmental features is important

It is important to observe that the T2I generator can manipulate not only the environmental features, but also the class-related ones. When the manipulated class-related features still resemble those of the original training set, the issue is alleviated. However, it is important for future generators to allow a stronger control on which features are manipulated and which not through language. In some cases, a potential solution could be to provide a mask that indicates which are the environmental features to be manipulated. To

Table 21. Inpainting Result on ImageNet-9

	in	mixed rand	mixed same	gap
ERM	95.06	71.85	83.58	11.73
OURS(H/D)	95.06	77.65	85.8	8.15
Inpaint(H)	96.05	80.62	87.16	6.54

Table 22. Dataset Statistics

	No.train	No.validation	No.test	No.classes
PACS	8977	1014	9991	7
Officehome	14032	1556	15588	65
ImageNet-9	2835	405	810	9
Texture	9600	1600	1280	16
CelebA-sub	5000	500	1000	2

exemplify the importance of controlling mainly the environmental variables, we show that, when the inpainting capabilities of Stable Diffusion can leverage ground-truth background masks to preserve the foreground area, this further improves the performance of our method on ImageNet-9 as shown in Tab. 21

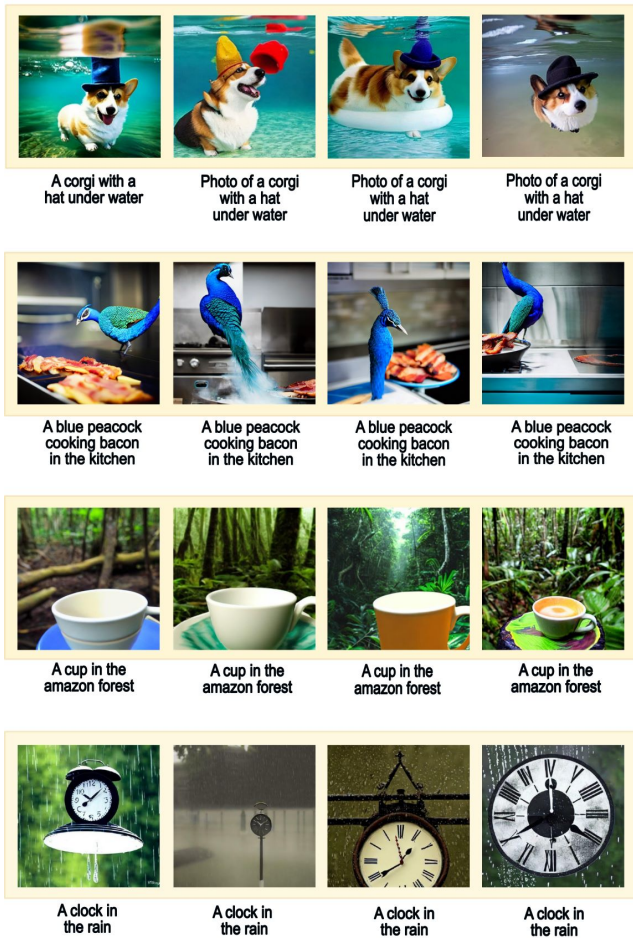
F. Augmentation Samples

F.1. Qualitative examples of generated samples vs retrieved samples

To argue that T2I generators can combine the known concepts in ways that are different from the ones observed in the training distribution, we compare some samples obtained from the generator and query an information retrieval system¹¹ that searches over LAION 5B (a super-set of the LAION Aesthetics dataset on which Stable Diffusion was trained). On the left side of Fig. 3, we show the generated images using prompts that combine several concepts; and on the right, we show the results obtained from the search engine. Since the dataset we are querying is huge, it is infeasible to give a certain answer about whether a sample representing the query is present or not in it. Additionally,

¹¹Search Engine can be accessed through <https://rom1504.github.io/clip-retrieval>

Generated Images



Search Engine Results



Figure 3. Comparison between Search Engine retrieval result and Stable Diffusion manipulation results. Images on the left are generated with Stable Diffusion; images on the right are retrieved from LAION-5B by querying the search engine with the prompt indicated below

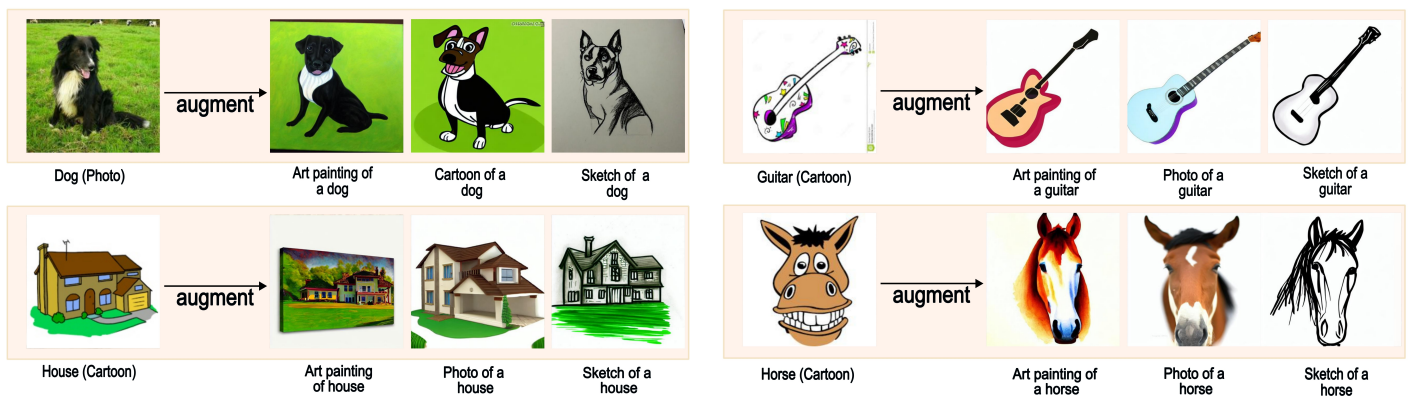


Figure 4. Stable Diffusion manipulation for in-distribution samples with prompt indicated below. For each group of images of four, the first image on the left is the original image, and the rest three are manipulated images



Figure 5. Stable Diffusion manipulation out-distribution samples with prompt indicated below. For each group of images of four, the first image is generated with prompt indicated from scratch, and the rest three are manipulated base on that.



Figure 6. Augmentation samples with VQGAN-CLIP, samples are shown in the same format as in Fig. 4

the system leverages CLIP embeddings to search for images similar to the query, so small differences in queries sometimes return highly variable results. For this reason, we try a variety of queries in an attempt to return images similar to the one that the generator produced to increase our confidence about the absence of a given image. Subjectively, we were unable to find images that reflected the compositional meaning of the prompts as well as those generated by Stable Diffusion. (See our discussion in Sec. 4 for our interpretation of these results.)

F.2. Qualitative examples of the augmented images

In Fig. 5 we show it is possible to intervene not only on images that resemble those that are likely to be in-domain (e.g., consider the first four rows), but also on figures that are out of the training distribution of the generator (obtained as discussed in the previous paragraph). We also show examples of augmentations obtained using VQGAN-CLIP in Fig. 6. As it can be seen, although the VQGAN-CLIP images resemble the original figure more, they also result in low-quality manipulations. On the other hand, Stable Diffusion, besides manipulating some of the target images, also manipulates the class-related images. We leave to future research devising a mechanism to address this issue (e.g., exploring the application of [23]).

F.3. The more the (synthetic) data, the better?

While in our framework the diversity of interventional samples is controlled by prompting strategy, a natural question is whether generating more samples can be beneficial. Therefore, for the PACS experiment, we ablate the amount of images we generate for each target domain (see Fig. 8) using Minimal prompts and Stable Diffusion. As it can be seen, increasing the amount of generated images up to 6 per-domain produces a 1.52% increase in the performance. Adding more data seems to degrade the performance. We leave to future work understanding whether this is due to the shift induced by the inevitable artifacts or low-quality images that might be produced when increasing the amount of generated samples or by the potentially low variety in the generated results.

F.4. Qualitative examples of failures

In Fig. 7 we present three failure cases of Stable Diffusion. In the first row, we observe Stable Diffusion fails at manipulating histological input images from the Camelyon-17 [2] and the RxRx1 [54] datasets. Camelyon-17 images contain tumoral and non-tumoral tissue captured in different environments. Since the changes between domains are hard to describe through language, we use Text inversion in order to learn how to transform from the source to the

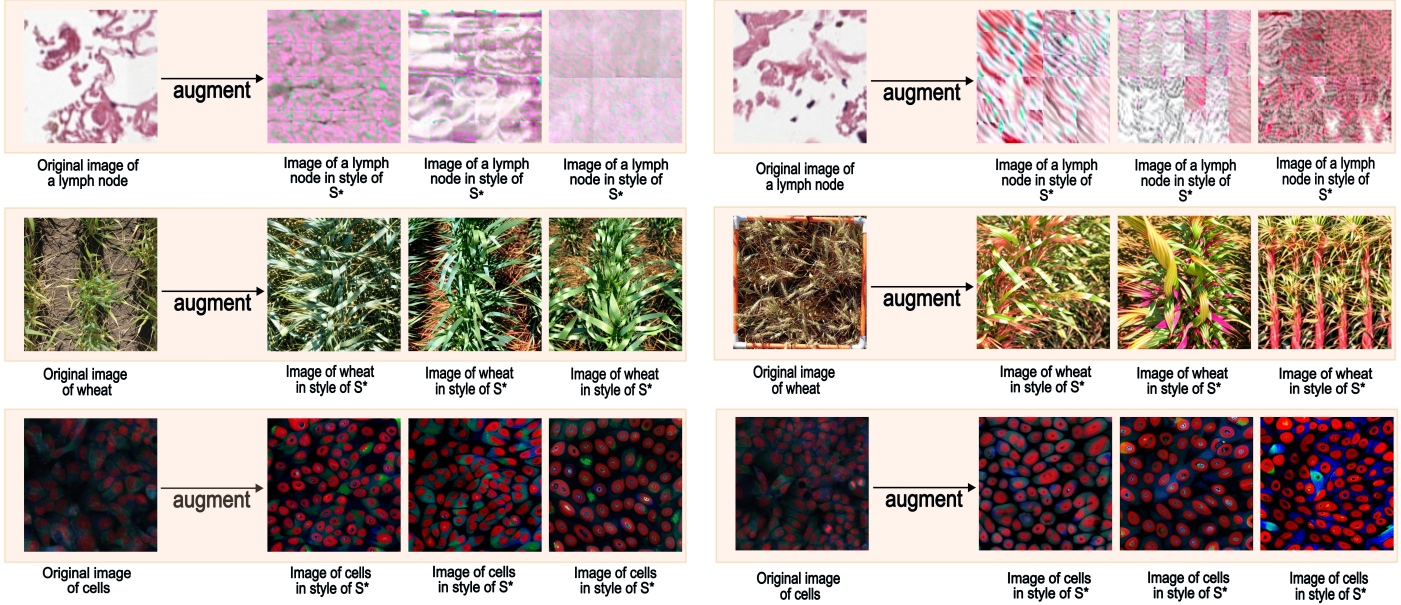


Figure 7. Text Inversion manipulation results for dramatically out-of-distribution data to Stable Diffusion training domain, as a domain adaptation approach. For each case, four sample images are randomly selected from the target test domain, and a style token S_* is learnt with text inversion and used as a style prompt to augment the original training domain image. Images are manipulated with the Text Inversion prompt from the left first original image in each group of four images. The samples from top to bottom are 1) Histological image from Camelyon-17 [2] 2) Cell image from RxRx1 [54] 3) Wheat image from GlobalWheat [8,9].

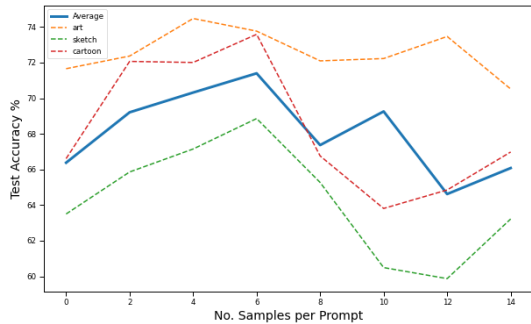


Figure 8. Number of samples generated for each prompt against test accuracy. The test accuracy is based on OURS(M/D) with ResNet-18 trained on Photo source domain.

target domains. As it can be seen, Stable Diffusion fails to produce realistic samples in this setting, probably because the input images and text are significantly out-of-domain. A less severe failure occurs on RxRx1 (second row), which represents HUVEC cells. In this case, the generated images still result in a distortion of the input that makes them unrealistic. For the GlobalWheat [8,9] dataset, it is apparent that while Stable Diffusion can generate plants but it does not reproduce the specific species depicted in the original in-

put and sometimes produces completely unrealistic instantiations of plants. This failure is particularly bad considering its training set contains several images of wheat crops; however, in those images, the crops are not captured from the angle in which they are captured in GlobalWheat (thus inducing a distribution shift). These failures suggest future research should be directed towards improving the ability of T2I generators to manipulate only the environmental variables for out-of-domain data, under the assumption a few text and image pairs from these unknown domains can be leveraged.

G. Lipschitzness

Bounding the Lipschitzness is not enough The authors of [32] proved that using Spectral Normalization on ResNets induces bi-Lipschitz constraints. Upper bounding the sensitivity of a model has been often correlated with improved generalization properties [50,65]. The underlying assumption is that covariate-shift perturbations reside within an \mathcal{L}_p -normed perturbation ball of the original distribution, and hence bounding the network’s variation in the output under such perturbations would maintain the in-domain accuracy. While in a few cases, this seems to have a positive effect (e.g., consider how well a model trained on the Art domain generalizes to Sketches, or a Photo does to

Cartoons in Table Tab. 8), this does not yield consistently better results for other types of domain changes (e.g., consider how the generalization of SN is worse than ERM on the Photo domain for a model trained on the Art domain).

H. Alternative Training Procedures

We also investigate an alternative contrastive way of leveraging the (real, augmented) image pairs. Since augmentations preserve the class label, the representation of an image pair should be similar regardless of the difference in environmental variables. Based on this idea, we investigate a contrastive (1) cosine similarity (2) l_2 loss between the original and augmented image pairs and combine it with the standard cross entropy loss for training. The experiment results are shown in Tab. 20. We obtain no significant improvement applying these techniques, therefore in the main paper, we use standard cross-entropy training with no additional contrastive terms.

I. Image-Generation Prompts

I.1. PACS

1. Minimal: { 'art painting': ['an art painting of'], 'sketch': ['a sketch of'], 'cartoon': ['a cartoon of'], 'photo': ['a photo of'] }
2. Hand-crafted: 'art painting': ['an oil painting of', 'a painting of', 'a fresco of', 'a colourful painting of', 'an abstract painting of', 'a naturalistic painting of', 'a stylised painting of', 'a watercolor painting of', 'an impressionist painting of', 'a cubist painting of', 'an expressionist painting of', 'an artistic painting of'], 'sketch': ['an ink pen sketch of', 'a charcoal sketch of', 'a black and white sketch', 'a pencil sketch of', 'a rough sketch of', 'a kid sketch of', 'a notebook sketch of', 'a simple quick sketch of'], 'photo': ['a photo of', 'a picture of', 'a polaroid photo of', 'a black and white photo of', 'a colourful photo of', 'a realistic photo of'], 'cartoon': ['an anime drawing of', 'a cartoon of', 'a colorful cartoon of', 'a black and white cartoon of', 'a simple cartoon of', 'a disney cartoon of', 'a kid cartoon style of']
3. Language Enhancement Moderate/Conservative: Generate with hint and language model specified in Appendix C.1

PACS: prompt is set in format "[TEMPLATE] of [CLASS LABEL]"

I.2. OfficeHome

1. Minimal: 'Art': ['an art image of'], 'Clipart': ['a clipart image of'], 'Product': ['an product image of'], 'Real World': ['a real world image of']
2. Handcrafted: 'Art': ['a sketch of', 'a painting of', 'an artistic image of'], 'Clipart': ['a clipart image

of'], 'Product': ['an image without background of'], 'Real World': ['a realistic photo of']

3. Language Enhancement Moderate/Conservative: Generate with hint and language model specified in Appendix C.1

I.3. ImageNet-9

1. Hand-crafted:background: [" in a parking lot", " on a sidewalk", " on a tree root", " on the branch of a tree", " in an aquarium", " in front of a reef", " on the grass", " on a sofa", " in the sky", " in front of a cloud", " in a forest", " on a rock", " in front of a red-brick wall", " in a living room", " in a school class", " in a garden", " on the street", " in a river", " in a wetland", " held by a person", " on the top of a mountain", " in a nest", " in the desert", " on a meadow", " on the beach", " in the ocean", " in a plastic container", " in a box", " at a restaurant", " on a house roof", " in front of a chair", " on the floor", " in the lake", " in the woods", " in a snowy landscape", " in a rain puddle", " on a table", " in front of a window", " in a store", " in a blurred background"]

I.4. CelebA-sub

1. Hand-crafted experiment: "blonde": ["male"], "non-blonde": ["female"]

I.5. Texture

We apply Human-in-the-loop to iteratively improve the quality of prompt and augmentation in Texture dataset. We start with a set of heuristic prompt as original version. Then based on the image generated, we add more representative prompts to further diversity the texture features. As shown in Tab. 13, by iteratively improving prompts, we achieve a final **8.28%** improvement more than **5.44%** of the initial improvement with respect to ERM.

1. Hand-crafted Final Version: texture: ['pointillism', 'rubin statue', 'rusty statue', 'ceramic', 'vaporwave', 'stained glass', 'wood statue', 'metal statue', 'bronze statue', 'iron statue', 'marble statue', 'stone statue', 'mosaic', 'furry', 'corel draw', 'simple sketch', 'stroke drawing', 'black ink painting', 'silhouette painting', 'black pen sketch', 'quickdraw sketch', 'grainy', 'surreal art', 'oil painting', 'fresco', 'naturalistic painting', 'stylised painting', 'watercolor painting', 'impressionist painting', 'cubist painting', 'expressionist painting', 'artistic painting']

2. Hand-crafted Original Version: texture: ['corel draw', 'simple sketch', 'stroke drawing', 'black ink painting', 'silhouette painting', 'black pen sketch', 'quickdraw sketch', 'grainy', 'surreal art', 'oil painting', 'fresco', 'naturalistic painting', 'stylised painting', 'watercolor painting', 'impressionist painting', 'cubist painting', 'expressionist painting', 'artistic painting']